Notch increases the shedding of HB-EGF by ADAM12 to potentiate invadopodia formation in hypoxia

Begoña Díaz,[1] Angela Yuen,[1] Shinji Iizuka,[1] Shigeki Higashiyama,[2] and Sara A. Courtneidge[1]

[1]Cancer Center, Tumor Microenvironment Program, Sanford-Burnham Medical Research Institute, La Jolla, CA 92037
[2]Department of Cell Growth and Tumor Regulation, Proteo-Medicine Research Center, Ehime University, Toon City, Ehime 791-0295, Japan

Notch regulates cell–cell contact-dependent signaling and is activated by hypoxia, a microenvironmental condition that promotes cellular invasion during both normal physiology and disease. The mechanisms by which hypoxia and Notch regulate cellular invasion are not fully elucidated. In this paper, we show that, in cancer cells, hypoxia increased the levels and activity of the ADAM12 metalloprotease in a Notch signaling–dependent manner, leading to increased ectodomain shedding of the epidermal growth factor (EGF) receptor (EGFR) ligand heparin-binding EGF-like growth factor. Released HB-EGF induced the formation of invadopodia, cellular structures that aid cancer cell invasion. Thus, we describe a signaling pathway that couples cell contact–dependent signaling with the paracrine activation of the EGFR, indicating cross talk between the Notch and EGFR pathways in promoting cancer cell invasion. This signaling pathway might regulate the coordinated acquisition of invasiveness by neighboring cells and mediate the communication between normoxic and hypoxic areas of tumors to facilitate cancer cell invasion.

Introduction

The Notch pathway mediates cell contact–dependent signaling. Notch signaling is initiated by the binding of transmembrane proteins (receptor and ligand) expressed by adjacent cells (Wharton et al., 1985). Upon ligand binding, the Notch receptor becomes susceptible to two consecutive proteolytic cleavages. The first is mediated by TNF-converting enzyme (Brou et al., 2000; Mumm et al., 2000) and generates a cleaved transmembrane form of the Notch receptor, which then serves as a substrate for the γ-secretase complex, to release the intracellular domain of Notch by intramembrane regulated proteolysis (De Strooper et al., 1999). The intracellular domain of Notch translocates to the nucleus and binds nuclear effectors to regulate transcription (Petcherski and Kimble, 2000). Notch plays fundamental roles in development and adult tissue homeostasis, and its deregulation contributes to cancer progression (Ellisen et al., 1991). Activated Notch signaling in cancer promotes cell invasion (Sahlgren et al., 2008; Chen et al., 2010) and metastasis (Santagata et al., 2004; Yang et al., 2011) by mechanisms that are not fully understood. In both normal and pathological contexts, the Notch pathway is pleiotropic, and the output of Notch signaling is often determined by the cross talk with other signaling pathways (Guruharsha et al., 2012).

Notch signaling is activated by hypoxia (Gustafsson et al., 2005). Physiological hypoxia regulates embryonic development, modulates stem cell biology, and promotes angiogenesis (Keith and Simon, 2007). Pathological hypoxia is common within solid malignant tumors (Höckel et al., 1991; Vaupel et al., 1991) and promotes malignant progression (Young et al., 1988; Brizel et al., 1996; Höckel et al., 1996). The hypoxia-inducible factor 1α (HIF-1α) regulates the cellular response to hypoxia (Wang et al., 1995). During mouse development, HIF-1α regulates morphogenic processes involving cell migration and remodeling of the extracellular matrix, including formation of the placenta (Adelman et al., 2000), heart (Krishnan et al., 2008), neural crest cell migration (Compernolle et al., 2003), chondrogenesis, and bone formation (Amarilio et al., 2007; Provot et al., 2007). During pathological hypoxia, HIF-1α regulates malignant tumor growth (Maxwell et al., 1997; Kung et al., 2000), angiogenesis (Mazure et al., 1996; Maxwell et al., 1997), and metastasis (Hiraga et al., 2007; Liao

Correspondence to Begoña Díaz: bdiaz@sanfordburnham.org

Abbreviations used in this paper: ADAM, A disintegrin and metalloprotease; CM, conditioned medium; EGFR, EGF receptor; EMT, epithelial to mesenchymal transition; Fc, fragment crystallizable; GSI, γ-secretase inhibitor; HB-EGF, heparin-binding EGF-like growth factor; HIF-1α, hypoxia inducible factor 1α; qPCR, quantitative PCR; rRNA, ribosomal RNA; TPA, 12-*O*-tetradecanoylphorbol 13-acetate.

The Rockefeller University Press $30.00
J. Cell Biol. Vol. 201 No. 2 279–292
www.jcb.org/cgi/doi/10.1083/jcb.201209151

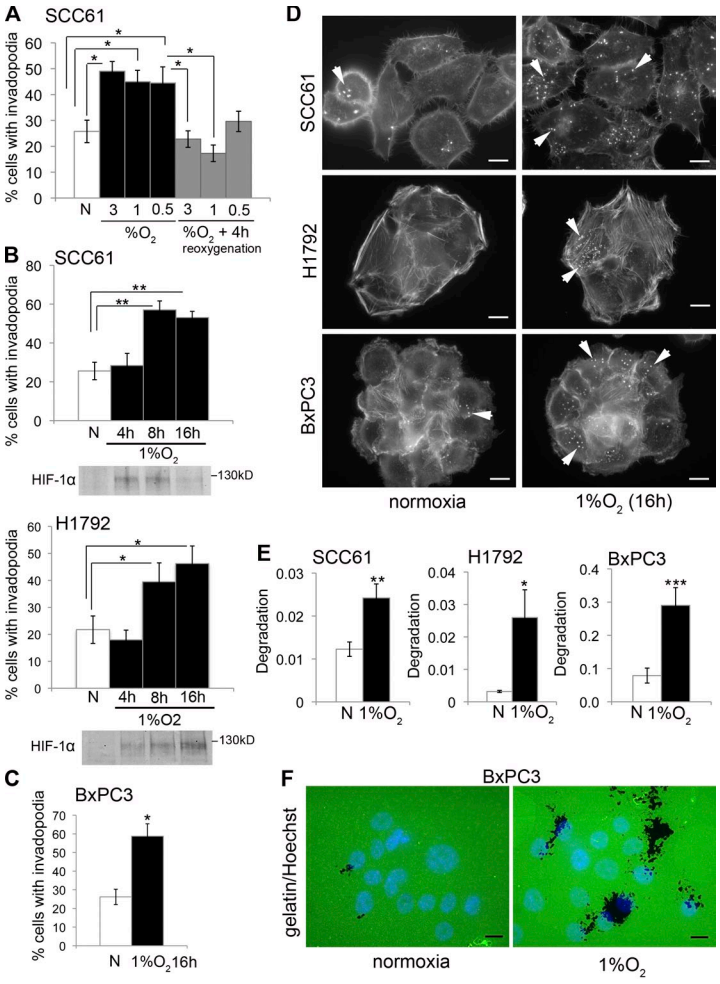

Figure 1. **Invadopodia formation is increased by hypoxia in human epithelial cancer cells.** (A) Cells forming invadopodia after 16 h at normoxia (N) or the indicated O_2 concentrations followed or not followed by 4 h of reoxygenation, $n = 2$. *, $P < 0.01$. (B) Cells forming invadopodia after hypoxia (1% O_2) for the indicated times or normoxia for 16 h, $n = 3$. *, $P < 0.01$; **, $P < 0.001$. HIF-1α protein levels upon treatment are shown. (C) Cells forming invadopodia after 16 h in normoxia or 1% O_2, $n = 3$. *, $P < 0.001$. (D) Cells stained for F-actin after treatment. Arrowheads, F-actin at invadopodia. (E) Invadopodia activity (degradation of labeled gelatin) after 16 h in normoxia or 1% O_2, $n = 3$. *, $P < 0.05$; **, $P < 0.01$; ***, $P < 0.005$. (F) Representative images of invadopodia activity of cells plated on gelatin (green) for 16 h in normoxia or 1% O_2. Nuclei, blue. Graphs show means ± SEM. Bars, 10 µm.

et al., 2007). The interplay between Notch, hypoxia, and HIF-1α in these contexts is only beginning to be addressed.

The heparin-binding EGF-like growth factor (HB-EGF; Higashiyama et al., 1991) activates ErbB1, also known as EGF receptor (EGFR), and ErbB4 by both juxtacrine and paracrine mechanisms. HB-EGF is synthesized as a membrane-anchored growth factor (pro-HB-EGF), which mediates juxtacrine signaling by binding to the receptor in neighboring cells (Higashiyama et al., 1995). In addition, protein ectodomain shedding of pro-HB-EGF by metalloproteases releases a soluble form of HB-EGF capable of activating the EGFR in a paracrine fashion (Goishi et al., 1995). HB-EGF potentiates tumor growth and angiogenesis (Miyamoto et al., 2004; Ongusaha et al., 2004) by mechanisms that are not fully understood. ADAM12, a member of the a disintegrin and metalloprotease (ADAM) family of proteases is a sheddase for pro-HB-EGF (Asakura et al., 2002). The ADAM12 metalloprotease is involved in myogenesis and adipogenesis in mice (Kurisaki et al., 2003), and its overexpression promotes orthotopic tumor growth in mice (Roy et al., 2011). ADAM12 expression is elevated in breast cancer and metastatic lymph nodes, bladder cancer, and lung carcinoma (Fröhlich et al., 2006; Rocks et al., 2006; Mino et al., 2009; Roy et al., 2011). The molecular mechanisms by which ADAM12 mediates these effects in cancer progression, including its role in cell invasion, are poorly understood.

Cell migration and invasion are fundamental for the patterning of the embryo as well as for immune surveillance and angiogenesis in the adult. Neural crest cells, macrophages, and vascular smooth muscle cells are examples of cell types implicated in these processes. All these cell types share the ability to form podosomes (Linder et al., 1999; Burgstaller and Gimona, 2005; Murphy et al., 2011), specialized regions of the plasma membrane containing adhesive and proteolytic enzymes that help cells to coordinate adhesion, migration, and pericellular proteolysis. Cancer cells form very similar structures termed invadopodia, which are associated with an invasive phenotype (Marchisio et al., 1984; Chen, 1989). Acquisition of invasive ability allows cancer cells to spread into surrounding tissues causing local invasion and also facilitates their spreading into distant organs to form metastasis. Both invasion and metastasis are hallmarks of cancer (Hanahan and Weinberg, 2011). Abrogating the ability of human cancer cells to form invadopodia greatly limits their migratory and/or invasive abilities (Seals et al., 2005; Clark et al., 2007), further indicating that these structures are important mediators of cancer cell invasiveness. The mechanisms that control invadopodia formation in the context of Actin polymerization and dynamics and the role of Actin-binding proteins have been extensively studied, and very important progress has been made (Weaver, 2006; Linder, 2007; Murphy and Courtneidge, 2011; Bravo-Cordero et al., 2012). However, many of the upstream signals that

regulate invadopodia (and podosome) formation and activity remain unknown. A better understanding of these regulatory pathways should greatly impact our knowledge of physiological and pathological cell invasion.

Here, we seek to investigate the regulation of cellular invasion by contact-dependent cellular signaling. We use cancer cells under hypoxia to understand how Notch signaling regulates cell invasion and describe a novel signaling pathway involving hypoxia, Notch, ADAM12, and HB-EGF that promotes invasiveness.

Results

Hypoxia potentiates the formation of functional invadopodia in epithelial tumor cells

Invadopodia formation is potentiated by hypoxia in the fibrosarcoma line HT-1080 (Lucien et al., 2011). To elucidate how general this cellular response is, we analyzed the formation of invadopodia under hypoxia in different cancer cell lines including SCC61 (head and neck), H1792 and H23 (lung), and BxPC3, PANC-1, and SU.86.86 (pancreas). We subjected SCC61 cells to different levels of hypoxia ranging from 0.5 to 3% O_2 for 16 h and analyzed the effect on the formation of invadopodia, which appear as small F-actin–rich dots (Fig. 1 D). Approximately 50% more cells formed invadopodia in all the hypoxic conditions tested, and the effect was reverted after 4 h of reoxygenation for cells growing under the less hypoxic conditions (Fig. 1 A). This indicated that maintenance of the hypoxic conditions is critical for the response. Because the different hypoxic conditions had a similar effect, we used 1% O_2 concentration, commonly used in vitro to model hypoxia, in this study.

Increased invadopodia formation by hypoxia in SCC61 and H1792 cells was not observed before 4 h, peaked at 8 h, and remained stable for ≤16 h in 1% O_2 (Fig. 1 B). The protein levels of the HIF-1α, a mediator of the cellular response to hypoxia, were already fully stabilized after 4 h in hypoxia (Fig. 1 B), but longer times were necessary to increase the number of cells forming invadopodia, suggesting a requirement for additional signaling events after HIF-1α stabilization. The observation that reoxygenation reverted the effect on invadopodia formation, and the fact that HIF-1α was still stabilized after 16 h in hypoxia (Fig. 1 B) further suggests that stabilized HIF-1α was necessary to increase invadopodia in these cells. BxPC3, H23, PANC-1, and SU.86.86 cells responded to hypoxia in a similar manner (Fig. 1, C and D; and Fig. S1, A, C, and D). Invadopodia induced by hypoxia were fully active as indicated by the increased ability of BxPC3, SCC61, and H1792 cells to focally degrade a layer of fluorescently labeled gelatin (Fig. 1, E and F; Fig. S1 B; and see Fig. 4 B).

HIF-1α is necessary for hypoxia-induced invadopodia formation

To assess the role of HIF-1α in hypoxia-induced invadopodia formation, we analyzed the ability of different cell lines to form invadopodia in hypoxia after transient transfection of two HIF-1α–specific siRNAs. Both oligonucleotides (oligos) efficiently blocked the accumulation of HIF-1α in hypoxia when compared with a nontargeting control as analyzed by immunoblotting (Fig. 2 A).

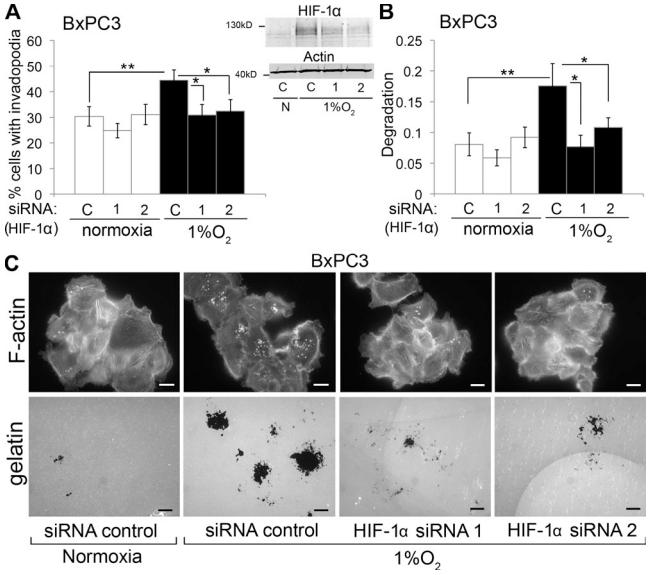

Figure 2. **Hypoxia-induced invadopodia formation requires HIF-1α.** (A, left) Cells forming invadopodia in normoxia (N) or 1% O_2 (16 h) after transfection with control (C) or HIF-1α siRNAs, $n = 3$. *, $P < 0.01$; **, $P < 0.05$. (right) HIF-1α protein levels after siRNA transfection. (B) Invadopodia activity (degradation) of cells after siRNA treatments and 16 h in normoxia or 1% O_2, $n = 2$. *, $P < 0.05$; **, $P < 0.005$. (C) Images from the experiment in A and B. Cells show F-actin at invadopodia (top) and were plated on fluorescent gelatin (bottom) to detect degradation. Graphs show means ± SEM. Bars, 18 µm.

Furthermore, the levels of the HIF-1α target gene *GLUT-1* (Chen et al., 2001) did not increase in hypoxia when cells were transfected with either HIF-1α siRNA (Fig. S2 B). Hypoxia no longer increased invadopodia formation after HIF-1α knockdown in BxPC3 cells (Fig. 2, A and C) and SCC61 cells (Fig. S2 A), although its knockdown did not affect the ability of the cells to form invadopodia in normoxia, in agreement with the specific role of HIF-1α in hypoxia. The HIF-1α inhibitor Echinomycin had a similar effect in hypoxia and a small but significant effect in normoxia (Fig. S2 C), perhaps by affecting additional targets. The increased ability of BxPC3 cells to degrade gelatin under hypoxia was also inhibited by silencing of HIF-1α (Fig. 2, B and C). These findings indicate a novel function for the HIF-1α transcription factor in promoting invadopodia formation in hypoxia.

Active Notch signaling mediates the increase in invadopodia formation in hypoxia

Hypoxia activates the Notch signaling pathway (Gustafsson et al., 2005). To analyze whether hypoxia activated Notch signaling in our cells, we measured the mRNA expression level of the Notch target gene *HES1* (*Hairy and enhancer of split 1*) by quantitative PCR (qPCR) and found that it was increased in SCC61, BxPC3, and H1792 cells after 16 h in hypoxia (Fig. 3 A and Fig. S3 D). To analyze whether Notch-dependent signaling regulated invadopodia formation under hypoxia, we treated cells with two different γ-secretase inhibitors (GSIs): GSI-IX, also known as DAPT (*N*-[(3,5-difluorophenyl)acetyl]-L-alanyl-2-phenyl]glycine-1, 1-dimethylethyl ester), and the equally selective but more potent

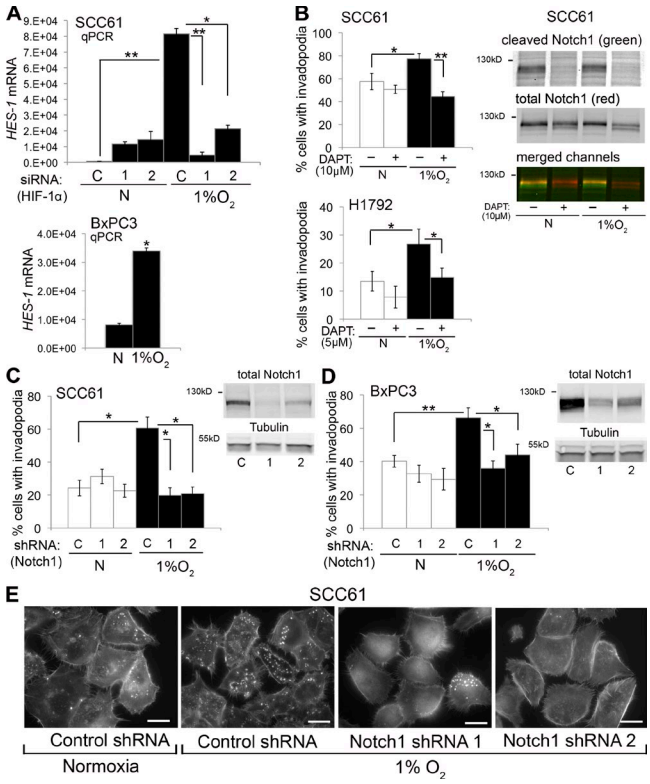

Figure 3. **Notch signaling mediates hypoxia-induced invadopodia formation.** (A, top) Means ± SD for *HES1* mRNA levels normalized to *18S* ribosomal RNA (rRNA) mRNA in cells transfected with control (C) or HIF-1α siRNAs after 16 h on normoxia (N) or 1% O_2, $n = 2$. *, $P < 0.05$; **, $P < 0.005$. (bottom) Means ± SD for *HES1* mRNA levels normalized to *Actin* mRNA after 16 h of in normoxia or 1% O_2, $n = 2$. *, $P < 0.05$. (B) Cells forming invadopodia after treatment with DAPT or vehicle in normoxia or 1% O_2 for 16 h, $n = 3$ for each cell line. *, $P < 0.05$; **, $P < 5 \times 10^{-5}$. (top right) Active (cleaved) NOTCH1 and total NOTCH1 protein levels in cells treated as indicated. (C, left) Cells expressing control or NOTCH1 shRNAs forming invadopodia after 16 h in normoxia or 1% O_2, $n = 3$. *, $P < 0.0001$. (right) NOTCH1 protein level in cells expressing control or NOTCH1 shRNAs. (D, left) Cells expressing control or NOTCH1 shRNAs forming invadopodia after 16 h in normoxia or 1% O_2, $n = 3$. *, $P < 0.001$; **, $P < 5 \times 10^{-5}$. (right) NOTCH1 protein level in cells expressing control or NOTCH1 shRNAs. (E) F-actin staining after the indicated treatments from experiment in C. Graphs in B–D are means ± SEM. Bars, 10 µm.

GSI-XXI or compound E. As expected, the levels of S3-cleaved (active) NOTCH1 were decreased by DAPT in SCC61 (Fig. 3 B). Treatment with DAPT abolished the increase in invadopodia formation under hypoxia in SCC61, H1792, PANC-1, and BxPC3 cells (Fig. 3 B and Fig. S2 D). Compound E had a similar effect (Fig. S2, E and F). The effect of GSI treatment on invadopodia formation in normoxia was lower than in hypoxia, indicating that a hypoxia-specific signaling pathway mediated by Notch increased the formation of invadopodia.

Components of the Notch signaling pathway in vertebrates comprise four transmembrane receptors (Notch 1–4) and five transmembrane ligands (JAG [JAGGED] 1 and 2 and DLLs [Delta-like ligands] 1, 3, and 4). All were expressed in SCC61 cells, and all but *JAG1*, *DLL1*, and *DLL4* were expressed in H1792 cells, as measured by RT-PCR (Fig. S4 A). Because the active form of Notch1 interacts with HIF-1α before recruitment to Notch-responsive promoters in the nuclei (Gustafsson et al., 2005), we investigated whether NOTCH1, which is expressed in SCC61, BxPC3, and H1792 cells (Fig. 3, C and D; and Fig. S3 E), was an effector of hypoxia in regulating invadopodia formation.

We generated SCC61, H1792, and BxPC3 cell lines stably expressing two different shRNA sequences that efficiently targeted NOTCH1 (Fig. 3, C and D; and Fig. S3 E). NOTCH1 knockdown rendered all of the cell lines studied refractory to increased invadopodia formation upon hypoxia (Fig. 3, C–E; and Fig. S3, E and F) but had minimal effects on the formation of invadopodia in normoxia. A similar effect was observed after transient transfection of SCC61 and BxPC3 with two different siRNAs targeting NOTCH1, ruling out possible off-target effects (Fig. S3, A–C). Consistent with its effect on invadopodia formation, NOTCH1 silencing also diminished the ability of SCC61 and BxPC3 to degrade gelatin in hypoxia, restoring its level to that of normoxia (Fig. 4, A and B; and Fig. S3 C). Although SCC61 and H1792 cells also express the NOTCH2 receptor, knockdown of NOTCH2 had no effect on invadopodia formation in these cells (Fig. S4, B and C). This result, along with the fact that NOTCH1 knockdown recapitulated the effect of GSI inhibitors, indicated specificity for NOTCH1 versus other Notch receptors in hypoxia-induced invadopodia formation in the cancer cell lines tested.

We observed that hypoxia increased the amount of mRNA for the Notch ligand *JAG2* in SCC61 cells in a HIF-1α–dependent manner (Fig. 4 C), consistent with previous observations in breast cancer cells (Xing et al., 2011). This may be part of the mechanism increasing Notch signaling under hypoxia. In agreement with this possibility, inducing the activation of Notch signaling in normoxia led to an increase in invadopodia formation to a level similar to that observed under hypoxia (Fig. 4 D and Fig. S4, D and E). We activated Notch in normoxia by plating cells on coverslips covered with recombinant JAG2 ligand, mimicking Notch-induced cell contact–dependent signaling (Sahlgren et al., 2008). The increase in invadopodia formation by active Notch signaling in normoxia was inhibitable by DAPT and not synergistic with hypoxia (Fig. 4 D and Fig. S4, D and E), indicating that active Notch signaling is necessary and sufficient to drive invadopodia formation. Furthermore, silencing of *JAG2* in SCC61 and H1792 cells abolished the effect of hypoxia on invadopodia formation (Fig. 4 E and Fig. S4 F), further indicating that cell contact–dependent signaling mediated by the Notch pathway promotes the formation of invadopodia under hypoxia.

Hypoxia increases the levels of the metalloprotease ADAM12 in a Notch-dependent manner

To gain insight into the downstream mechanism by which cell contact–dependent signaling promotes invadopodia formation, we first analyzed whether the effect of hypoxia on invadopodia formation was mediated by a cell-autonomous or a non–cell-autonomous mechanism. We collected conditioned media (CM) from SCC61 or BxPC3 cells growing in hypoxia for 16 h and added it to cells in normoxia. CM from hypoxic, but not from normoxic, cells induced an increase in invadopodia formation after 6 h of treatment (Fig. 5 A). This suggests that the effect of hypoxia on invadopodia formation in these cells is, at

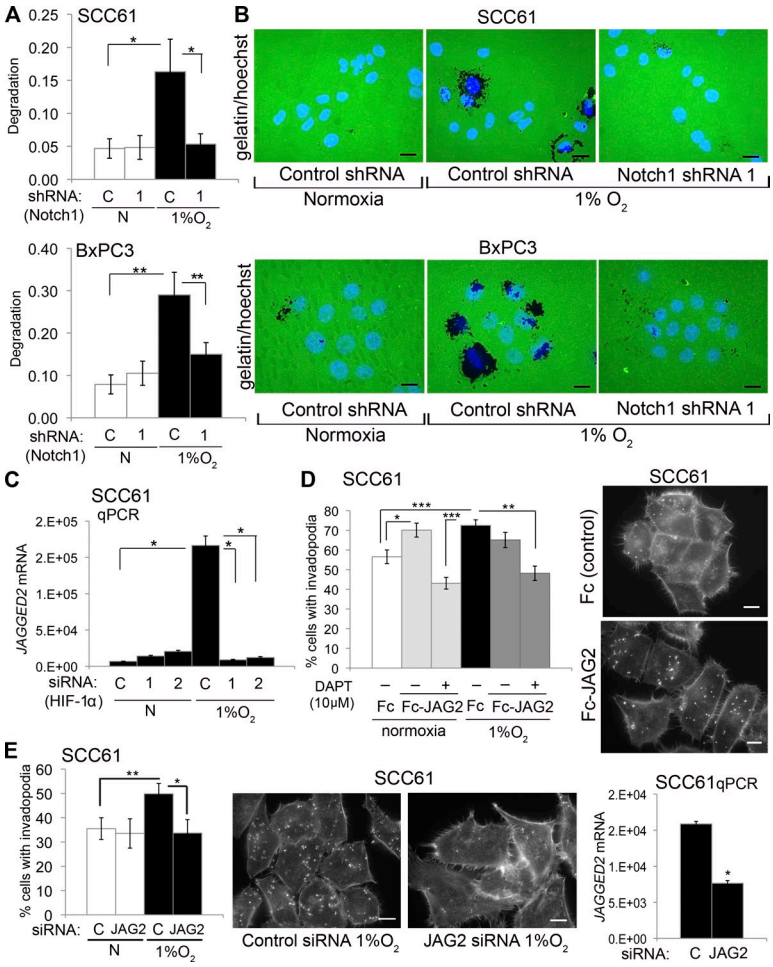

Figure 4. **Notch-induced cell contact–dependent signaling regulates invadopodia formation in hypoxia.** (A) Degradation of control (C) or NOTCH1 shRNAs cells incubated for 16 h in normoxia (N) or 1% O_2, $n = 3$ for each line. *, $P < 0.05$; **, $P < 0.005$. (B) Images from experiments in A of cells plated on green fluorescent gelatin and stained with Hoechst. (C) Means ± SD for *JAG2* mRNA levels normalized to *Actin* mRNA in cells transfected with control or HIF-1α siRNAs after 16 h on normoxia or 1% O_2, $n = 2$. *, $P < 0.01$. (D, left) Cells forming invadopodia after plating on control Fc or Fc-JAG2 and grown as indicated for 16 h, $n = 3$. *, $P < 0.01$; **, $P < 0.001$; ***, $P < 5 \times 10^{-5}$. (right) Representative images of cells plated on Fc or Fc-JAG2 in normoxia showing F-actin at invadopodia. (E, left) Cells forming invadopodia after transfection with control or JAG2 siRNA pool and 16 h in normoxia or 1% O_2, $n = 2$. *, $P < 0.01$; **, $P < 0.001$. (middle) Representative images of invadopodia-associated F-actin in cells from the same experiment. (right) Means ± SD for *JAG2* mRNA levels normalized to *18S* mRNA in cells transfected with control or JAG2 siRNA, $n = 2$. *, $P < 0.01$. Graphs in A, D, and E show means ± SEM. Bars, 10 μm.

least in part, mediated by a non–cell-autonomous mechanism. In a different set of experiments, the metalloprotease inhibitor GM6001 prevented the increase in invadopodia formation in hypoxia (Fig. 5 B). Collectively, these results suggested the implication of a non–cell-autonomous mechanism mediated by a metalloprotease in the induction of invadopodia by hypoxia. Candidates to mediate this effect are the ADAM family of proteases, which modulate signaling by regulated proteolysis of transmembrane proteins, including receptors, cell adhesion molecules, and growth factor precursors (Seals and Courtneidge, 2003). In support of a role for ADAM proteases in invadopodia formation under hypoxia, we observed a NOTCH1-dependent increase in *ADAM12* mRNA levels in SCC61 after 16 h in hypoxia (Fig. 5 C), which is consistent with a recent study showing that active Notch signaling in normoxia increases the levels of *Adam12* transcripts in mouse cells (Li et al., 2011). Our findings suggest that ADAM12 is an effector of hypoxia in cancer cells.

ADAM12 is necessary for invadopodia formation in hypoxia

To assess whether the increase in the amount of ADAM12 transcripts has functional relevance in invadopodia formation in hypoxia, we transfected SCC61 and H1792 cells with a pool of siRNAs targeting *ADAM12*. In both cases, *ADAM12* silencing abrogated the increase in invadopodia formation induced by hypoxia (Fig. S5, A and B). To rule out possible off-target effects, we generated cell lines stably expressing two different shRNA sequences specific for *ADAM12*. For both cell lines and with both independent shRNA sequences, we confirmed impairment in hypoxia-induced invadopodia formation when the levels of *ADAM12* remained low (Fig. 6, A and B; and Fig. S5 D). Invadopodia formation in normoxia was largely independent of ADAM12 in these cells. Furthermore, the effect of ADAM12 in invadopodia formation under hypoxia was mediated by a non–cell-autonomous mechanism because, unlike CM from control cells, CM from ADAM12 knockdown cells grown in hypoxia was not able to induce invadopodia formation when added to cells in normoxia (Fig. 6 C). Collectively, these data indicate that ADAM12, acting through a non–cell-autonomous mechanism, is necessary for invadopodia formation under hypoxia.

HB-EGF is necessary for hypoxia-induced invadopodia formation

ADAM12 mediates the ectodomain shedding of HB-EGF, a ligand for ErbB1 (EGFR) and ErbB4. HB-EGF is synthesized as a transmembrane protein (pro-HB-EGF) susceptible to ectodomain shedding, which releases soluble HB-EGF to the extracellular space. This process increases the availability of the ligand to the receptor in the same and/or in neighboring cells. We hypothesized that the Notch-dependent increase of ADAM12 in hypoxia may lead to increased ectodomain shedding of HB-EGF, which in turn would increase invadopodia formation.

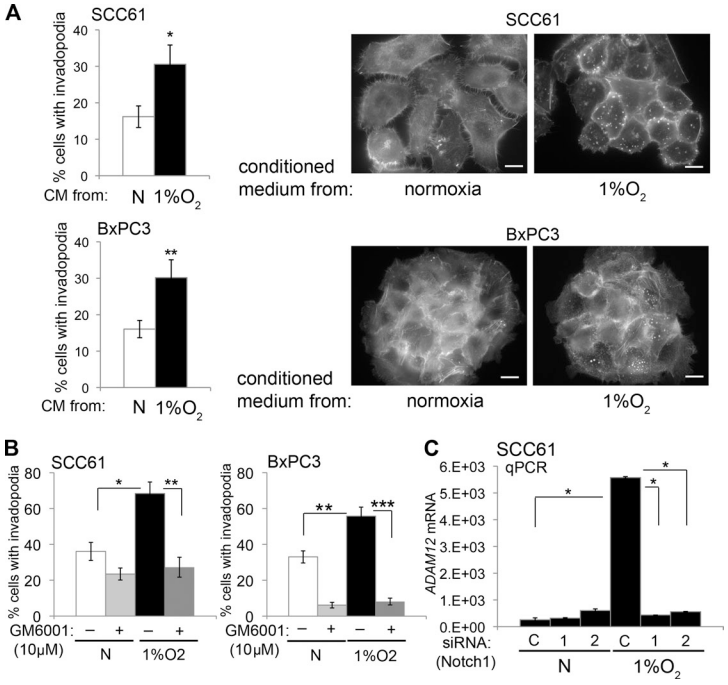

Figure 5. **Hypoxia regulates invadopodia formation through a non–cell-autonomous mechanism and induces ADAM12 levels.** (A, left) Cells forming invadopodia after 6 h of treatment in normoxia (N) with conditioned medium (CM) from cells grown in normoxia or 1% O_2 for 16 h, $n = 3$ for each cell line. *, $P < 0.005$; **, $P < 0.001$. (right) Invadopodia-associated F-actin in cells from the same experiments. (B) Cells forming invadopodia after treatment with the metalloprotease inhibitor GM6001 in normoxia or 1% O_2 for 16 h, $n = 2$ for each cell line. *, $P < 0.05$; **, $P < 0.0005$; ***, $P < 10^{-5}$. (C) Means ± SD of *ADAM12* mRNA levels normalized to *Actin* in cells transfected with control (C) or NOTCH1 siRNAs and cultured in normoxia or 1% O_2 for 16 h, $n = 3$. *, $P < 0.005$. Graphs in A and B show means ± SEM. Bars, 10 µm.

We first analyzed whether HB-EGF affected invadopodia formation. Treatment of SCC61, BxPC3, and H1792 cells with recombinant soluble HB-EGF increased the number of cells forming invadopodia in normoxia (Fig. 7, A and B). To analyze whether HB-EGF–dependent signaling affects hypoxia-induced invadopodia formation, we inhibited HB-EGF signaling by two independent methods. Treatment of cells with a specific HB-EGF–blocking antibody (Rubin et al., 1991) significantly reduced the number of cells forming invadopodia in hypoxia to a level similar to that of normoxia when compared with IgG control-treated cells (Fig. 7 C). In a second approach, we used the HB-EGF–specific inhibitor CRM-197, which binds and inhibits pro-HB-EGF and soluble HB-EGF but not EGF (Mitamura et al., 1995). Treatment of cells with CRM-197 had an effect comparable to the HB-EGF–blocking antibody in invadopodia formation under hypoxia (Fig. 7 D). Furthermore, inhibition of EGFR tyrosine kinase activity with Gefitinib also abrogated the increase in invadopodia formation in SCC61 and BxPC3 cells after hypoxia (Fig. 7 E), suggesting that activation of the EGFR by HB-EGF may mediate invadopodia formation in hypoxia. Whereas blockade of HB-EGF signaling had minimal effects on invadopodia formation in normoxia, inhibition of EGFR in SCC61

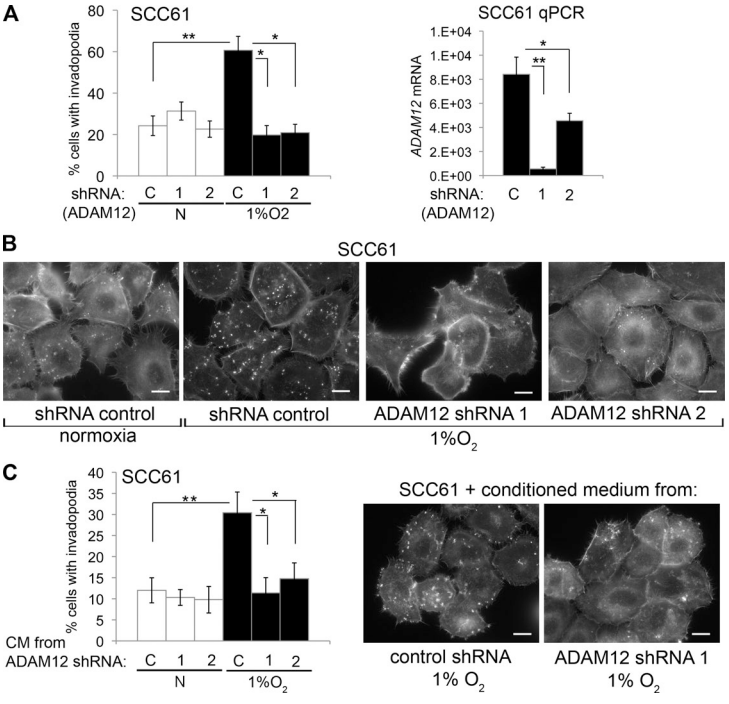

Figure 6. **ADAM12 is an effector of hypoxia-induced invadopodia formation acting through a non–cell-autonomous mechanism.** (A, left) Cells expressing control (C) or *ADAM12* shRNAs forming invadopodia after 16 h in normoxia (N) or 1% O_2, $n = 3$. *, $P < 0.01$; **, $P < 10^{-5}$. (right) Means ± SD of *ADAM12* mRNA levels normalized to *18S* rRNA in control or ADAM12 knockdown cell lines, $n = 2$. *, $P < 0.05$; **, $P < 0.01$. (B) Invadopodia-associated F-actin in cells quantified on the left in A. (C, left) Cells forming invadopodia after 6 h of treatment in normoxia with conditioned medium (CM) from control or ADAM12 knockdown cell lines grown in normoxia or 1% O_2 for 16 h, $n = 2$. *, $P < 0.005$; **, $P < 0.001$. (right) F-actin in cells from the same experiment. Graphs in A, B, and E show means ± SEM. Bars, 10 µm.

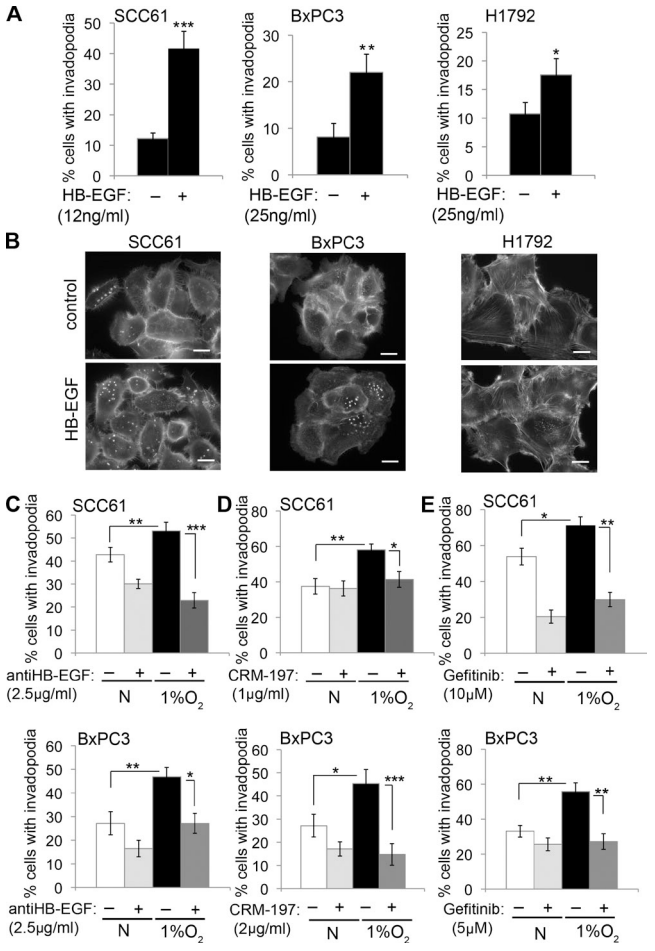

Figure 7. **HB-EGF mediates hypoxia-induced invadopodia formation.** (A) Cells forming invadopodia after treatment with HB-EGF for 6 h in normoxia, $n = 3$ for each cell line. *, $P < 0.05$; **, $P < 0.005$; ***, $P < 5 \times 10^{-5}$. (B) Invadopodia-associated F-actin in cells quantified in A. (C) Cells forming invadopodia after treatment with blocking HB-EGF antibody or IgG control for 16 h in normoxia (N) or 1% O_2, $n = 3$ for each cell line. *, $P < 0.05$; **, $P < 0.005$; ***, $P < 10^{-5}$. (D) Cells forming invadopodia after treatment with CRM-197 for 16 h in normoxia or 1% O_2, $n = 3$ for each cell line. *, $P < 0.05$; **, $P < 0.001$; ***, $P < 10^{-5}$. (E) Cells forming invadopodia after treatment with Gefitinib or vehicle for 16 h in normoxia or 1% O_2, $n = 3$ for each cell line. *, $P < 0.01$; **, $P < 0.005$. Graphs show means ± SEM. Bars, 10 µm.

also abrogated invadopodia formation in normoxia (Fig. 7 E), suggesting that SCC61 cells are highly dependent on EGFR signaling for invadopodia formation. Together, these results indicate that HB-EGF is an effector of hypoxia and that HB-EGF–dependent signaling is necessary and sufficient for hypoxia-induced invadopodia formation.

Hypoxia promotes ADAM12-dependent shedding of HB-EGF in a Notch-dependent manner

The increased levels of *ADAM12* mRNA in hypoxia, along with the requirements for both ADAM12 (in a non–cell-autonomous manner) and HB-EGF in invadopodia formation in hypoxia, provide strong circumstantial evidence that ADAM12-dependent HB-EGF shedding regulates hypoxia-induced invadopodia formation. In agreement with this, the metalloprotease inhibitor KB-R7785, a potent inhibitor of HB-EGF shedding that binds to ADAM12 (Asakura et al., 2002), diminished the effect of hypoxia in invadopodia formation in SCC61 cells (Fig. S5 C). To provide direct evidence in support of our hypothesis, we generated HB-EGF–shedding reporter cell lines stably expressing a chimeric HB-EGF protein fused to the enzymatic domain of human placental AP, referred to as AP tag HB-EGF (Tokumaru et al., 2000). Shedding of HB-EGF in these cells can be quantified by measuring the activity of AP in the CM. To analyze the effect of hypoxia in HB-EGF shedding, cells were cultured in normoxia or hypoxia for 16 h. Medium was replaced by fresh medium containing 12-*O*-tetradecanoylphorbol 13-acetate (TPA), an inducer of HB-EGF shedding (Goishi et al., 1995), and AP activity was measured in the CM after 1 h in normoxia. In agreement with our hypothesis, SCC61 or BxPC3 cells expressing AP-tagged HB-EGF exhibited a significant increase in HB-EGF shedding after hypoxia (Fig. 8, A and B). Treatment with the Notch inhibitor compound E decreased HB-EGF shedding after hypoxia, indicating that hypoxia-induced HB-EGF shedding is dependent on Notch activation (Fig. 8, A and B). In addition to the quantitative data obtained by measuring AP activity in the CM, we assessed the subcellular localization of the AP-tagged HB-EGF protein by immunofluorescence using an AP antibody. Whereas AP-tagged HB-EGF was largely localized to the plasma membrane in SCC61 cells cultured in normoxia, the protein was absent from the plasma membrane upon 16 h in hypoxia, consistent with the shedding of the AP-containing HB-EGF fragment from the cell surface (Fig. 8 C). When treated with the Notch inhibitor compound E in hypoxia, the AP-tagged HB-EGF protein was still retained at the plasma membrane in some cells (Fig. 8 C), consistent with the decreased shedding activity quantified previously (Fig. 8 A).

To further analyze the role of hypoxia-induced Notch signaling in the ADAM12-dependent shedding of HB-EGF in cancer cells, we measured the shedding of HB-EGF under normoxia or hypoxia in SCC61 cells after knockdown of ADAM12, NOTCH1, or JAG2 with siRNA pools. The increase in the shedding of HB-EGF under hypoxia was prevented by the knockdown of each protein (Fig. 8 D), further indicating that the shedding of HB-EGF by ADAM12 is regulated by hypoxia in a Notch signaling–dependent manner.

The expression of ADAM12 is elevated in hypoxic areas of malignant tumors

Our results indicate that ADAM12 is an effector of hypoxia in cancer cells. To explore the physiological relevance of this finding, we searched genomic databases for the expression of *HIF-1α* and *ADAM12* in normal versus lung cancer tumor samples. The comparison of 15 independent analyses, on a total of 256 normal and 456 lung cancer samples, indicated that both *ADAM12* and *HIF-1α* were frequently overexpressed in tumor samples (Fig. 9 A). A representative analysis (Hou et al., 2010) revealed overexpression gene ranks of top 14% for *HIF-1α* and top 4% for *ADAM12* (Fig. 9 B). Because the regulation of HIF-1α is mainly posttranscriptional (Ohh et al., 2000), we analyzed the expression of HIF-1α and ADAM12 by immunohistochemistry on lung tumor sections. The expression of ADAM12 was increased

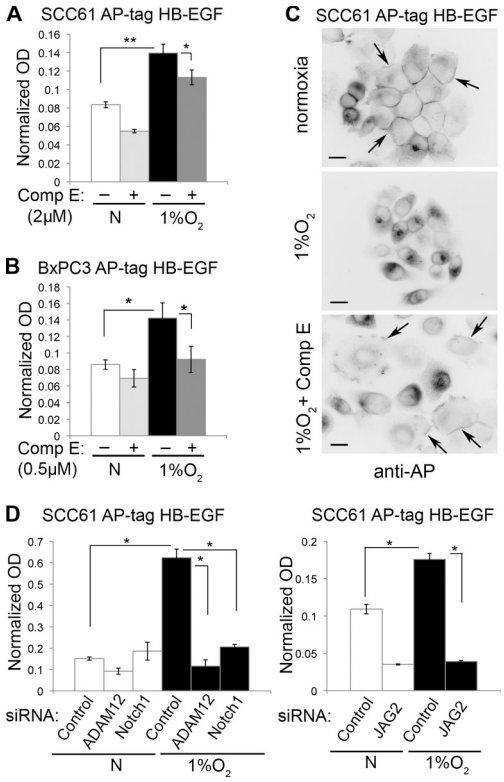

Figure 8. **Hypoxia induces HB-EGF ectodomain shedding in a NOTCH-dependent manner.** (A) HB-EGF shedding of SCC61 AP-tagged HB-EGF cells in normoxia (N) or 1% O_2 for 16 h. Graphs represent means ± SD of AP activity values in the CM, $n = 4$. *, $P < 0.01$; **, $P < 0.0005$. (B) HB-EGF shedding of BxPC3 AP-tagged HB-EGF cells cultured in normoxia or 1% O_2 for 16 h. Graph represent means ± SD of AP activity values, $n = 3$. *, $P < 0.0005$. (C) AP-tagged HB-EGF subcellular localization (anti-AP) after the indicated treatments. Arrows point to cells with plasma membrane-localized AP–HB-EGF. Bars, 10 µm. (D, left) HB-EGF shedding of SCC61 AP-tagged HB-EGF cells transfected with the indicated siRNAs control after 16 h in normoxia or 1% O_2, $n = 4$. (right) HB-EGF shedding of SCC61 AP-tagged HB-EGF cells transfected with control or JAG2 siRNA and cultured in normoxia or 1% O_2 for 16 h, $n = 2$. Graphs show means ± SD for AP activity. *, $P < 0.001$. Comp E, compound E.

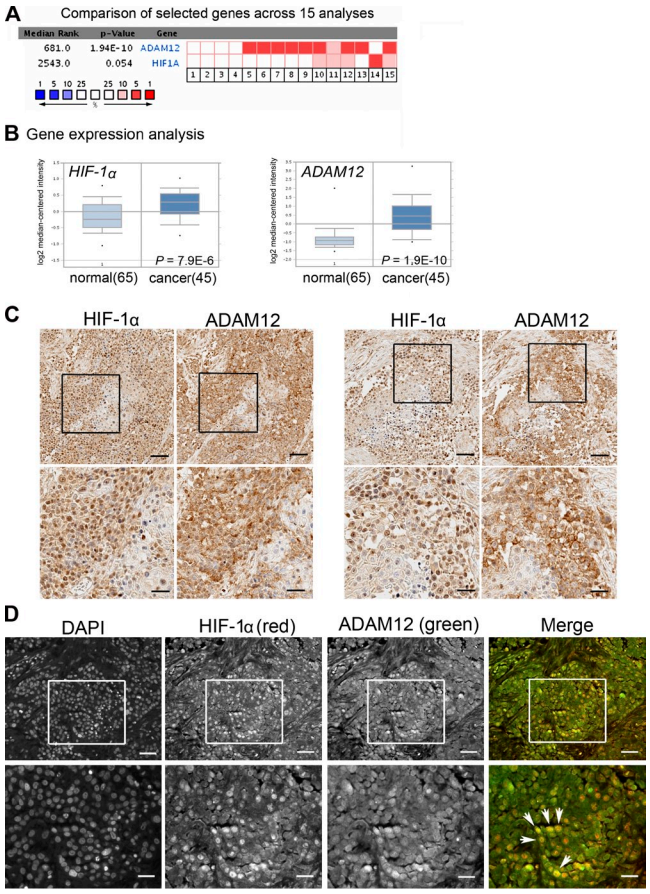

Figure 9. **HIF-1α and ADAM12 expression in human tumor samples.** (A) Oncomine was used to compare *HIF-1α* and *ADAM12* expression across 15 independent analyses of normal versus tumor lung samples. Color scale represents over- or underexpression ranks. (1–4) Bhattacharjee et al. (2001); (5–8) Garber et al. (2001); (9 and 10) Hou et al. (2010); (11) Landi et al. (2008); (12) Stearman et al. (2005); (13) Su et al. (2007); (14) Talbot et al. (2005); (15) Wachi et al. (2005). (B) Box and whisker plots for *HIF-1α* and *ADAM12* gene expression from analysis 9 in A. Dots are maximum and minimum values, lines are the medians, boxes are 75th and 25th percentiles, and whiskers are the 90th and10th percentiles. (C) Immunohistochemistry for HIF-1α and ADAM12 in consecutive sections of different areas of a lung cancer tumor sample. Bottom images are magnifications of the areas in squares. Bars: (top) 100 µm; (bottom) 25 µm. (D) Costaining for HIF-1α and ADAM12 on sections from the same tumor. Bottom images are magnifications of the areas in squares. Arrows, cells with strong colocalization of HIF-1α and ADAM12 signals. Bars: (top) 75 µm; (bottom) 30 µm.

in areas of high nuclear HIF-1α staining when compared with areas of very low or undetectable nuclear HIF-1α, as detected in tumor samples from three independent donors (Fig. 9 C shows two different areas of one representative tumor). Costaining revealed frequent colocalization of ADAM12 staining in cells expressing high levels of nuclear HIF-1α (Fig. 9 D). These results indicated that ADAM12 is overexpressed in hypoxic areas of malignant tumors and suggest that ADAM12 is an effector of hypoxia in cancer cells in vivo.

Collectively, our results indicate that cell–cell communication regulates the proinvasive response of cells to hypoxia by coupling contact-dependent signaling mediated by Notch, with paracrine signaling mediated by the release of HB-EGF and the activation of the EGFR. These findings point to ADAM12 as an effector of hypoxia and HB-EGF as an effector of Notch. We propose a model (Fig. 10) in which contact-dependent signaling mediated by Notch activates paracrine (as well as autocrine and juxtacrine) signaling through the ADAM12-dependent release of HB-EGF and activation of the EGFR. Hypoxia is revealed here as an instructive signal that induces a non–cell-autonomous proinvasive response within a given cancer cell population through the interplay between cell contact–dependent and paracrine signaling.

Discussion

Cell invasion is fundamental for some biological processes, including patterning of the embryo and adult immune surveillance. Although invasive ability is restricted for most cells in adult tissues, that restriction is lost in cancer, in which normally noninvasive cell types acquire invasiveness and spread into surrounding tissues. Although important progress has been made in understanding the cell-autonomous pathways that regulate cell invasiveness, the non–cell-autonomous pathways are less well understood.

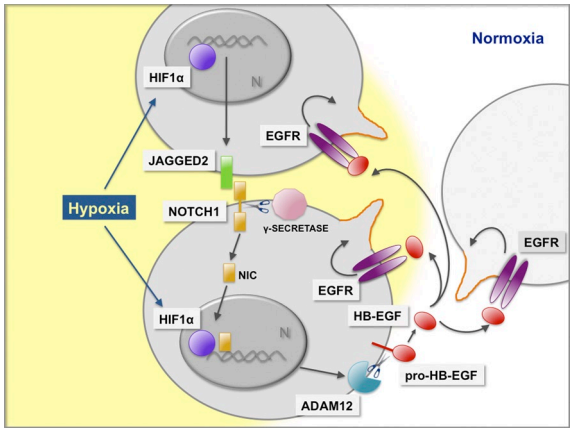

Figure 10. **Proposed model for increased invadopodia formation through Notch-dependent shedding of HB-EGF by ADAM12 downstream hypoxia.** In cells within hypoxic areas (yellow), the levels of HIF-1α are stabilized, and Notch signaling is activated, at least in part, by increasing the levels of the ligand JAG2. After ligand to receptor binding, the γ-secretase complex cleaves NOTCH1 releasing the intracellular domain of the NOTCH1 fragment (NIC) that translocates to the nucleus (N) of the signal-receiving cell. Activated Notch increases ADAM12 levels, whose activity induces the ectodomain shedding of pro-HB-EGF. Released HB-EGF binds to EGF receptors (EGFR) in the same, adjacent, or distant cells. Activation of EGFR by HB-EGF leads to increased formation of invadopodia (orange). Paracrine signaling through HB-EGF released by hypoxic cells may promote invadopodia formation in cells located in normoxic regions (white), which suggest cross talk between normoxic and hypoxic areas of tumors.

The integration of cell-autonomous and non–cell-autonomous pathways underlies the regulation of invasiveness at the cell population level.

We describe here a signaling pathway that regulates invasiveness by coupling cell contact–dependent signaling (mediated by hypoxia-activated Notch) with the paracrine activation of the EGFR (mediated by the ADAM12-dependent release of HB-EGF). We propose that this pathway represents a mechanism by which cells acquire the coordinated ability to invade during cancer. We further hypothesize that normal cells might use a similar mechanism to invade in a coordinated manner during physiological invasion. Furthermore, this mechanism might mediate the cross talk between normoxic and hypoxic regions of tumors to regulate collective cell invasion.

Contact-dependent signaling and cancer cell invasion

Pathological hypoxia promotes cancer cell invasion and metastasis (Young et al., 1988; Brizel et al., 1996; Höckel et al., 1996), and Notch is an effector of hypoxia in different types of cancer cells, including melanoma (Bedogni et al., 2008), breast cancer (Chen et al., 2010), and lung cancer (Chen et al., 2007). However, the signaling mechanisms by which hypoxia and Notch interact are far from understood. Most Notch receptors and ligands are expressed by both tumor and stromal cells and, therefore, may mediate either homotypic signaling between cancer cells or heterotypic signaling between cancer cells and tumor stromal cells. For instance, JAG1 in cancer cells binds to receptors on endothelial cells to promote tumor angiogenesis (Zeng et al., 2005) or to receptors on the metastatic bone stroma to promote bone metastasis (Sethi et al., 2011). The specific role of homotypic Notch signaling in vivo has been more difficult to dissect because inhibition of Notch signaling by GSIs targets both tumor and stroma, and activation of Notch by overexpressing the full-length or cleaved (active) form of the receptor often bypasses the need for ligand binding. Using an in vitro system, we show that homotypic Notch signaling is both necessary and sufficient to increase the formation of invadopodia and therefore to promote cell invasiveness.

Our results indicate a positive role for NOTCH1 in cancer invasion. Although oncogenic mutations in human NOTCH1 have been described in hematological malignancies (Weng et al., 2004), recent studies describe putative tumor-suppressive mutations in cutaneous and lung carcinomas (Wang et al., 2011) and in a subset of head and neck carcinomas (Agrawal et al., 2011; Stransky et al., 2011). Although the tumor-suppressive effect of these mutations remains to be experimentally tested, the effects of Notch are clearly context dependent. For instance, decreasing Notch signaling with GSI treatment has therapeutic effects in a KRas-driven mouse model of lung cancer (Maraver et al., 2012), whereas genetic ablation of the Notch effector CSL in the normal skin mesenchymal compartment promotes field cancerization, thus increasing the risk of skin cancer in mice (Hu et al., 2012). The cross talk between Notch and other signaling pathways in both physiological and pathological contexts is fundamental to the outcome of Notch signaling. We show here that the Notch pathway and the EGFR pathway are coupled during hypoxia to drive invadopodia formation. This provides a contextual framework in which NOTCH1 potentiates cell invasion.

Cross talk between Notch and EGFR pathways through ADAM12 function

ADAM12 and HB-EGF are revealed here as novel effectors of hypoxia in cellular invasion. The role of ADAM12 in promoting invadopodia under hypoxia is in agreement with studies showing that ADAM12 contributes to tumor growth and metastasis in orthotopic breast tumor xenografts (Roy et al., 2011) as well as tumor growth in a mouse model of prostate cancer (Peduto et al., 2006). Furthermore, ADAM12 is a candidate breast cancer gene (Sjöblom et al., 2006), is overexpressed in malignant breast tissue and metastatic lymph nodes (Kveiborg et al., 2005; Lendeckel et al., 2005; Roy et al., 2011), human glioblastoma (Kodama et al., 2004), lung adenocarcinoma (Rocks et al., 2006), and head and neck cancer (Roepman et al., 2005; Markowski et al., 2009), and is a prognostic factor in resected lung adenocarcinoma (Mino et al., 2009). However, the mechanisms by which ADAM12 affects cancer progression remain largely unknown. Our finding that ADAM12 activity is increased by hypoxia in tumor cells and potentiates the formation of invadopodia provides a mechanism to explain its ability to facilitate invasion and metastasis and indicates that ADAM12 levels and activity may be regulated by microenvironmental conditions. Although the knockdown of *ADAM12* had minimal effects on invadopodia formation in normoxia, treatment with GM6001, which inhibits HB-EGF shedding (Miyamoto et al., 2004; Xu et al., 2004; Wang et al., 2007), also affected invadopodia formation in normoxia, albeit to a lower extent. This is in agreement with a previous study (Clark et al., 2007) and may reflect the inhibition of additional GM6001 targets

in normoxia. ADAM12 binds to the invadopodia component Tks5, localizes to invadopodia in Src-transformed mouse fibroblasts (Abram et al., 2003), and translocates to the plasma membrane upon phosphorylation by Src (Stautz et al., 2010). It is possible that ADAM12 localizes to invadopodia in cancer cells through binding to Tks5 and/or Src and promotes the local shedding of HB-EGF at invadopodia, as suggested previously (Albrechtsen et al., 2011). Further investigation will help understand the interplay between endogenous ADAM12 and invadopodia as well as the suggested role of invadopodia as sites of localized ectodomain shedding activity.

We describe that ADAM12-mediated shedding of HB-EGF is increased under hypoxia in a Notch-dependent manner and that released HB-EGF mediates invadopodia formation by EGFR-dependent signaling. HB-EGF has been shown to be highly expressed in different tumor tissues, including pancreatic ductal adenocarcinomas (Wang et al., 2007). Furthermore, HB-EGF is overexpressed in breast cancer cells that specifically metastasize to the brain (Bos et al., 2009). Soluble HB-EGF increased the number of cells forming invadopodia, and inhibition of HB-EGF by CRM-197 reverted the effect. Consistent with a positive role of HB-EGF in tumor progression, different studies describe the antitumoral effects of CRM-197 (Dateoka et al., 2012; Tang et al., 2012). HB-EGF is likely to affect invadopodia formation through binding to EGFR because Gefitinib inhibited the increase in invadopodia formation induced by hypoxia. Inhibition of EGFR with Gefitinib, but not inhibition of HB-EGF by a blocking antibody or CRM-197 treatment, inhibited invadopodia formation in normoxia, indicating that other EGFR ligands mediated EGFR signaling in invadopodia in normoxia. Indeed, EGF induces invadopodia formation through EGFR signaling in rat mammary adenocarcinoma cells (Yamaguchi et al., 2005). The specific signaling mechanisms by which HB-EGF induces invadopodia formation remain to be analyzed.

Although ADAM12 is the main sheddase for HB-EGF (Asakura et al., 2002; Sahin et al., 2004), some pancreatic cancer cell lines, including the BxPC3 cells used in this study, do not have detectable levels of *ADAM12*. However, these cells still displayed increased shedding of HB-EGF, which was necessary for hypoxia-induced invadopodia formation downstream of Notch. This raises the question of which protease is responsible for HB-EGF shedding after hypoxia in pancreatic cells lacking ADAM12 expression. Candidates are ADAM15 and ADAM9, which are highly expressed in pancreatic tumors (Yamada et al., 2007). Further experiments will be necessary to characterize the potential role of these ADAM family members as mediators of hypoxia-induced invadopodia formation.

Notch, invadopodia, and epithelial to mesenchymal transition (EMT) in cancer

Hypoxia and NOTCH signaling promote migration and invasion of cancer cells through the stabilization of Snail-1 and the induction of EMT (Sahlgren et al., 2008). Invadopodia might underlie these effects in invasion because they are induced by Snail and Twist-1 (Eckert et al., 2011). Several components of the pathway we described play a role in EMT, including Notch (Zavadil et al., 2004) and HB-EGF (Wang et al., 2007). Furthermore, TGF-β, which induces EMT, up-regulates *ADAM12* transcripts in human liver cells (Le Pabic et al., 2003). We have not observed clear evidence of EMT in any of the cell lines subjected to hypoxia for 16 h, perhaps because longer times are required for hypoxia to induce EMT (Lester et al., 2007; Sahlgren et al., 2008) or perhaps because of differences in the susceptibility to EMT of the cell lines used. However, we cannot rule out the possibility that a program of EMT has been already activated after 16 h of hypoxia in our cells. Further investigation will be needed to elucidate the relationship between the induction of invadopodia under hypoxia and the process of EMT in cancer.

The relevance of nonautonomous signaling mechanisms to regulate cell invasion

The mechanisms that mediate cell–cell communication within tumors are largely unknown. If the signaling pathway we describe here operates inside tumors, as suggested by the expression of ADAM12 in hypoxic areas of lung tumor sections, hypoxia-mediated Notch activation might lead to the synchronized acquisition of invasive ability by groups of cancer cells. It is tempting to speculate that the formation of invadopodia in a synchronized manner (through cell contact–dependent signaling mediated by Notch) may be a mechanism underlying the phenomenon of collective cell invasion (Friedl et al., 2012).

Whereas invadopodia formation in the hypoxic regions of a tumor would directly depend on the hypoxic conditions, the release of soluble HB-EGF by cells in hypoxia might induce the formation of invadopodia in normoxic cells at a distance from the hypoxic region (determined by the diffusion limit of HB-EGF). Indeed, the hypoxic core of tumors is often located at a distance from the invasive front. This mechanism might mediate the cross talk between the hypoxic and normoxic regions of a tumor to potentiate cellular invasion in a non–cell-autonomous manner. In that context, hypoxia would be an instructive signal able to induce synchronized invasiveness to distant cells in normoxia.

In summary, we propose a complex signaling pathway that regulates cell invasiveness in a non–cell-autonomous manner by coupling cell contact–dependent signaling and paracrine signaling downstream hypoxia. These findings have important implications in understanding cell–cell communication and the regulation of cancer cell invasion.

Materials and methods

Cell lines

SCC61 cells (head and neck squamous cell carcinoma) were obtained from A. Weaver (Vanderbilt University Medical Center, Nashville, TN) and grown in DMEM containing 20% FBS and 4 µg/ml hydrocortisone (Sigma-Aldrich); NCI-H1792 and NCI-H23 lung cancer cells (a gift from J. Minna and A. Gazdar, University of Texas Southwestern, Dallas, TX) and BxPC3 pancreatic cancer cells (purchased from American Type Culture Collection) were grown in RPMI 1640 containing 10% FBS. PANC-1 and SU.86.86 pancreatic cancer cells (purchased from American Type Culture Collection) were grown in DMEM containing 10% FBS. FBS was obtained from HyClone. RPMI 1640 and DMEM (4.5 g/liter glucose) were purchased from Corning. All experiments were performed in complete medium in the absence of antibiotics.

Hypoxia treatment

Unless otherwise stated, cells were incubated for 16 h in a 1% O_2 and 5% CO_2 atmosphere in a humidified chamber in an incubation system (Xvivo; BioSpherix).

Reagents and antibodies
DAPT was purchased from Tocris Bioscience, TPA was purchased from Sigma-Aldrich, Echinomycin and compound E were obtained from Enzo Life Sciences, GM6001 was obtained from EMD, CRM-197 was obtained from BioAcademia, Gefitinib was purchased from Selleck Chemicals, and recombinant human HB-EGF was obtained from R&D Systems. Primary antibodies were HIF-1α (BD for immunoblotting and Novus Biologicals for immunohistochemistry), Notch1 (D1E11) and active Notch1 (D3B8; both obtained from Cell Signaling Technology), placental AP (H-330; Santa Cruz Biotechnology, Inc.), HB-EGF (AF-259; R&D Systems), ADAM12 (Proteintech), and γ-tubulin (Sigma-Aldrich). Goat IgG control was obtained from Santa Cruz Biotechnology, Inc. Alexa Fluor 568–conjugated phalloidin and Alexa Fluor 594– or Alexa Fluor 488–conjugated goat secondary antibodies for immunofluorescence were obtained from Invitrogen.

RNAi and treatment with inhibitors
siRNA oligos targeting HIF-1α (J-004018-08 and J004018-10), NOTCH1 (J-007771-10 and J-007771-12), NOTCH2 (pool, J-0171870-00-0005), ADAM12 (pool, L005118-00-0005), and JAG2 (pool, L-012235-00-0005) as well as nontargeting controls were obtained from Thermo Fisher Scientific. siRNA oligos were transfected at 20 nM (individual) or 80 nM (pools) using Lipofectamine 2000 (Invitrogen). 48 h later, cells were trypsinized and counted, and 4×10^4 cells were seeded on 18-mm glass in 12-well plates, transferred to hypoxia, and processed for invadopodia quantification or activity 16 h later. For RNA or protein extraction, $5–7 \times 10^5$ cells were plated in 60-mm dishes, transferred to hypoxia, and processed 16 h later. shRNA lentiviral constructs targeting NOTCH1 (TRCN0000350330 and TRCN0000003359) and ADAM12 (TRCN0000047033 and TRCN0000047034) were obtained from Sigma-Aldrich. Lentiviral particles were generated by the Sanford Burnham Medical Research Institute (SBMRI) viral vector shared resource. After lentiviral infection, cells were selected with Puromycin (ECM Biosciences) at a final concentration of 5 µg/ml (SCC61) or 2 µg/ml (H1792 and BxPC-3) for 7–10 d before performing the experiments. Treatment with inhibitors was performed at the time of plating.

DNA constructs
The AP-tagged HB-EGF–expressing construct was described before (Tokumaru et al., 2000). A fragment containing the AP-tagged HB-EGF–encoding DNA was subcloned into the lentiviral expression construct pCDH-CMV-MCS-EF1-neomycin (System Biosciences). Lentiviral particles were generated by the SBMRI viral vector shared resource. Cells were selected with G418 (ECM Biosciences) at a final effective concentration of 300 µg/ml for SCC61 cells and 400 µg/ml for BxPC3 cells for 7–10 d before performing experiments.

Immunoblotting
For HIF-1α immunoblotting, the nuclear fraction was extracted by lysing cells in a hypotonic NP-40–based lysis buffer for 30 min on ice. The lysate was spun 5 min at 2,500 rpm at 4°C, and the pellet containing nuclei was washed five times with the same lysis buffer. The pellet was then resuspended in a hypertonic lysis buffer, incubated 30 min on ice, and spun 15 min at 14,000 rpm at 4°C. Samples were separated in 8% polyacrylamide gels (Invitrogen). For NOTCH1 immunoblotting, cells were lysed in a Triton X-100–based lysis buffer. Cleared lysate was assayed for total protein content using the bicinchoninic acid protein assay (Thermo Fisher Scientific), and 80–100 µg of total protein per sample was separated in an 8% polyacrylamide gel (Invitrogen). Secondary antibodies were conjugated to Alexa Fluor 680 (Invitrogen) or IR800 (Rockland Immunochemicals), and membranes were scanned using an infrared imaging system (Odyssey; LI-COR Biosciences).

RNA extraction and qPCR
RNA was extracted with RNeasy kit (QIAGEN). cDNA synthesis was performed using a reverse transcriptase kit (SuperScript III First-Strand; Invitrogen). qPCR was performed by the SBMRI Gene Analysis Core facility using qPCR SuperMix power SYBR green (Applied Biosystems) and a real-time cycler (Mx3000P; Agilent Technologies). Actin or 18S mRNAs were used as normalizers.

Invadopodia detection and gelatin degradation assay
Cells were fixed in 4% PFA (Electron Microscopy Sciences) in PBS for 20 min at RT, incubated in 3% BSA and 0.1% Triton X-100 in PBS for 30 min at RT, and incubated with Alexa Fluor 568–conjugated phalloidin (1:100–1:500 in PBS containing 0.3% BSA and 0.1% Triton X-100) for 1 h at RT. For each independent experiment, the number of cells forming invadopodia was quantified in ≥15 microscope fields (40×) imaged randomly and representing a total of ∼150 cells per experimental condition. For gelatin degradation assays, sterile coverslips were coated with a thin layer of Oregon green gelatin obtained from Invitrogen (0.2 mg/ml in PBS containing 2% sucrose), fixed in 0.5% glutaraldehyde for 15 min, washed in PBS, and incubated with 5 mg/ml sodium borohydride for 3 min at RT. After washing in PBS, coverslips were transferred to sterile multiwell plates and incubated in complete growth medium for 30 min at 37°C. Cells were plated on top and incubated in normoxia or hypoxia as indicated. After processing for F-actin staining, images were randomly taken at 40× for ≥15 fields per experiment. The percentage of degraded area normalized to the number of nuclei in that area was represented as "degradation." The percentage of degraded area was quantified with ImageJ (National Institutes of Health).

Treatment with CM
SCC61 (2×10^5 cells per well) or BxPC3 (1.5×10^5 cells per well) were plated in 24-well plates in 0.5 ml of growing media and transferred to hypoxia or left in normoxia for 16 h. Medium was collected, spun, and immediately used to treat cells for 6 h in normoxia. Cells were processed for invadopodia staining, and invadopodia numbers were quantified.

Notch activation
Notch was activated by using immobilized recombinant human JAG2 according to a previous protocol with some modifications (Sahlgren et al., 2008). Glass coverslips were coated overnight at RT with 100 µg/ml recombinant protein G (Invitrogen) in PBS. After three washes in PBS, coverslips were blocked with 10 mg/ml BSA in PBS for 2 h at RT, washed with PBS, and incubated with recombinant human JAG2 fragment crystallizable (Fc) chimera (R&D Systems) or purified human IgG Fc fragment (EMD Millipore) at 2 µg/ml in PBS containing 1 mg/ml BSA for 4–6 h at RT. Coverslips were washed, and cells (4×10^4) were plated on top and incubated in normoxia in the presence of DAPT or DMSO. After 16 h, cells were processed for quantification of invadopodia.

Immunofluorescence
AP staining was performed in the absence of detergents. Cells were fixed in 4% PFA. The AP antibody was used at 1:200 dilution overnight at 4°C. Cells were washed and incubated 1 h in PBS containing 0.3% BSA and 1:500 dilution of Alexa Fluor 488–conjugated anti–rabbit antibody.

Microscopy
Fluorescence microscopy images were obtained with a fluorescent microscope (Axioplan 2; Carl Zeiss) equipped with a charge-coupled device camera (AxioCam HRm; Carl Zeiss) and AxioVision software (Carl Zeiss). Images were acquired at RT at either 40 or 63× using Plan Neofluar 40×/0.75 NA or Plan Apochromat 63×/1.40 NA oil differential interference contrast objectives, respectively. Images in Fig. 8 were inverted using Photoshop (Adobe).

Shedding experiments
Shedding experiments were performed essentially as previously described (Tokumaru et al., 2000) with minor modifications. AP–HB-EGF–expressing cells were plated in 24-well plates (10^5 cells per well for SCC61; 1.5×10^5 cells per well for BxPC3) and transferred to hypoxia (1% O_2) 5 h after plating. After 16 h on hypoxia, cells were washed three times in PBS and incubated in 0.5 ml DMEM with 4.5 g/liter glucose without phenol red (Invitrogen) containing 60 nM TPA for 1 h in normoxia. CM was collected and spun for 5 min at 14,000 rpm. AP activity in the CM was assayed immediately using an AP activity kit (BioVision) in 80–100 µl of sample in quadruplicate in a 96-well assay plate. Incubation was performed at 37°C in the dark until color developed. Colorimetry was performed using an absorbance microplate reader (ELx800; BioTek Instruments, Inc.) with absorbance set at 405 nm. For normalization, each well containing cells was lysed in 100 µl Triton X-100–based lysis buffer, and protein content in the cleared lysate was calculated using the bicinchoninic acid assay. Colorimetric values for AP activity were normalized to the protein content (micrograms per milliliter) of the cells in the corresponding well. When indicated, cells were treated with inhibitors or vehicle at the time of plating, and fresh inhibitors or vehicle was added to the shedding media containing TPA. For siRNA experiments, cells were transfected 48 h before plating and assayed for AP activity 60 h after transfection.

Statistical analysis
All experiments were reproduced at least three times with similar results. In the figure legends, *n* is the number of experimental replicates averaged in a graph. Statistical significance was determined by calculating the p-value using the paired Student's *t* test.

Bioinformatics

The Oncomine database (Compendia Bioscience) was used to compare gene expression profiles for *HIF-1α* and *ADAM12* between normal and lung cancer samples. The rank of a gene is the median rank for that gene across each of the analyses, and the p-value for a gene is the p-value for the median-ranked analysis. P-values were calculated by Oncomine using Student's *t* test.

Immunohistochemistry

Lung tumor samples embedded in paraffin were obtained from the SBMRI tumor bank. Adjacent tumor sections were stained with HIF-1α or ADAM12 antibodies (1:50) according to manufacturer's instructions. Signal was developed with DAB or Alexa Fluor 488– or Alexa Fluor 546–conjugated antibodies. Slides were digitalized using slide scanner (ScanScope XT; Aperio), and images were exported as JPEGs.

Online supplemental material

Fig. S1 shows quantification of invadopodia in H23, H1792, PANC-1, and SU.86.86 cells. Fig. S2 shows quantification of invadopodia and *GLUT1* mRNA levels in SCC61 after HIF-1α siRNA transfection, quantification of invadopodia after Echinomycin treatment on SCC61, and GSI treatment on PANC-1, SCC61, and BxPC3 cells. Fig. S3 shows quantification of invadopodia after Notch1 siRNA transfection on SCC61, H1792, and BxPC3 cells. Fig. S4 shows expression of Notch signaling pathway components in SCC61 and H1792 cells, effect of Notch2 knockdown on invadopodia formation in hypoxia, and invadopodia quantification after activation of Notch by recombinant JAG2 in BxPC3 and H1792 cells and, after JAG2 siRNA treatment, in H1792 cells. Fig. S5 shows quantification of invadopodia after ADAM12 siRNA in SCC61 and H1792 cells and, after ADAM12 shRNA, in H1792 cells. Online supplemental material is available at http://www.jcb.org/cgi/content/full/jcb.201209151/DC1. Additional data are available in the JCB DataViewer at http://dx.doi.org/10.1083/jcb.201209151.dv.

We are grateful to A. Weaver, J. Minna, and A. Gazdar for their gifts of cell lines. We thank the SBMRI Stem Cell, Viral Vector, Gene Analysis, and Histopathology Core Facilities for their excellent technical support. We also thank C. Abdullah for his help with HIF-1α siRNA experiments at the beginning of this project.

Funding was obtained from National Institutes of Health CA129686, CA153065, and CA154002 to S.A. Courtneidge.

Submitted: 28 September 2012
Accepted: 15 March 2013

References

Abram, C.L., D.F. Seals, I. Pass, D. Salinsky, L. Maurer, T.M. Roth, and S.A. Courtneidge. 2003. The adaptor protein fish associates with members of the ADAMs family and localizes to podosomes of Src-transformed cells. *J. Biol. Chem.* 278:16844–16851. http://dx.doi.org/10.1074/jbc.M300267200

Adelman, D.M., M. Gertsenstein, A. Nagy, M.C. Simon, and E. Maltepe. 2000. Placental cell fates are regulated in vivo by HIF-mediated hypoxia responses. *Genes Dev.* 14:3191–3203. http://dx.doi.org/10.1101/gad.853700

Agrawal, N., M.J. Frederick, C.R. Pickering, C. Bettegowda, K. Chang, R.J. Li, C. Fakhry, T.X. Xie, J. Zhang, J. Wang, et al. 2011. Exome sequencing of head and neck squamous cell carcinoma reveals inactivating mutations in NOTCH1. *Science*. 333:1154–1157. http://dx.doi.org/10.1126/science.1206923

Albrechtsen, R., D. Stautz, A. Sanjay, M. Kveiborg, and U.M. Wewer. 2011. Extracellular engagement of ADAM12 induces clusters of invadopodia with localized ectodomain shedding activity. *Exp. Cell Res.* 317:195–209. http://dx.doi.org/10.1016/j.yexcr.2010.10.003

Amarilio, R., S.V. Viukov, A. Sharir, I. Eshkar-Oren, R.S. Johnson, and E. Zelzer. 2007. HIF1alpha regulation of Sox9 is necessary to maintain differentiation of hypoxic prechondrogenic cells during early skeletogenesis. *Development.* 134:3917–3928. http://dx.doi.org/10.1242/dev.008441

Asakura, M., M. Kitakaze, S. Takashima, Y. Liao, F. Ishikura, T. Yoshinaka, H. Ohmoto, K. Node, K. Yoshino, H. Ishiguro, et al. 2002. Cardiac hypertrophy is inhibited by antagonism of ADAM12 processing of HB-EGF: metalloproteinase inhibitors as a new therapy. *Nat. Med.* 8:35–40. http://dx.doi.org/10.1038/nm0102-35

Bedogni, B., J.A. Warneke, B.J. Nickoloff, A.J. Giaccia, and M.B. Powell. 2008. Notch1 is an effector of Akt and hypoxia in melanoma development. *J. Clin. Invest.* 118:3660–3670. http://dx.doi.org/10.1172/JCI36157

Bhattacharjee, A., W.G. Richards, J. Staunton, C. Li, S. Monti, P. Vasa, C. Ladd, J. Beheshti, R. Bueno, M. Gillette, et al. 2001. Classification of human lung carcinomas by mRNA expression profiling reveals distinct adenocarcinoma subclasses. *Proc. Natl. Acad. Sci. USA*. 98:13790–13795. http://dx.doi.org/10.1073/pnas.191502998

Bos, P.D., X.H. Zhang, C. Nadal, W. Shu, R.R. Gomis, D.X. Nguyen, A.J. Minn, M.J. van de Vijver, W.L. Gerald, J.A. Foekens, and J. Massagué. 2009. Genes that mediate breast cancer metastasis to the brain. *Nature*. 459:1005–1009. http://dx.doi.org/10.1038/nature08021

Bravo-Cordero, J.J., L. Hodgson, and J. Condeelis. 2012. Directed cell invasion and migration during metastasis. *Curr. Opin. Cell Biol.* 24:277–283. http://dx.doi.org/10.1016/j.ceb.2011.12.004

Brizel, D.M., S.P. Scully, J.M. Harrelson, L.J. Layfield, J.M. Bean, L.R. Prosnitz, and M.W. Dewhirst. 1996. Tumor oxygenation predicts for the likelihood of distant metastases in human soft tissue sarcoma. *Cancer Res.* 56:941–943.

Brou, C., F. Logeat, N. Gupta, C. Bessia, O. LeBail, J.R. Doedens, A. Cumano, P. Roux, R.A. Black, and A. Israël. 2000. A novel proteolytic cleavage involved in Notch signaling: the role of the disintegrin-metalloprotease TACE. *Mol. Cell*. 5:207–216. http://dx.doi.org/10.1016/S1097-2765(00)80417-7

Burgstaller, G., and M. Gimona. 2005. Podosome-mediated matrix resorption and cell motility in vascular smooth muscle cells. *Am. J. Physiol. Heart Circ. Physiol.* 288:H3001–H3005. http://dx.doi.org/10.1152/ajpheart.01002.2004

Chen, C., N. Pore, A. Behrooz, F. Ismail-Beigi, and A. Maity. 2001. Regulation of glut1 mRNA by hypoxia-inducible factor-1. Interaction between H-ras and hypoxia. *J. Biol. Chem.* 276:9519–9525. http://dx.doi.org/10.1074/jbc.M010144200

Chen, J., N. Imanaka, J. Chen, and J.D. Griffin. 2010. Hypoxia potentiates Notch signaling in breast cancer leading to decreased E-cadherin expression and increased cell migration and invasion. *Br. J. Cancer*. 102:351–360. http://dx.doi.org/10.1038/sj.bjc.6605486

Chen, W.T. 1989. Proteolytic activity of specialized surface protrusions formed at rosette contact sites of transformed cells. *J. Exp. Zool.* 251:167–185. http://dx.doi.org/10.1002/jez.1402510206

Chen, Y., M.A. De Marco, I. Graziani, A.F. Gazdar, P.R. Strack, L. Miele, and M. Bocchetta. 2007. Oxygen concentration determines the biological effects of NOTCH-1 signaling in adenocarcinoma of the lung. *Cancer Res.* 67:7954–7959. http://dx.doi.org/10.1158/0008-5472.CAN-07-1229

Clark, E.S., A.S. Whigham, W.G. Yarbrough, and A.M. Weaver. 2007. Cortactin is an essential regulator of matrix metalloproteinase secretion and extracellular matrix degradation in invadopodia. *Cancer Res.* 67:4227–4235. http://dx.doi.org/10.1158/0008-5472.CAN-06-3928

Compernolle, V., K. Brusselmans, D. Franco, A. Moorman, M. Dewerchin, D. Collen, and P. Carmeliet. 2003. Cardia bifida, defective heart development and abnormal neural crest migration in embryos lacking hypoxia-inducible factor-1alpha. *Cardiovasc. Res.* 60:569–579. http://dx.doi.org/10.1016/j.cardiores.2003.07.003

Dateoka, S., Y. Ohnishi, and K. Kakudo. 2012. Effects of CRM197, a specific inhibitor of HB-EGF, in oral cancer. *Med. Mol. Morphol.* 45:91–97. http://dx.doi.org/10.1007/s00795-011-0543-6

De Strooper, B., W. Annaert, P. Cupers, P. Saftig, K. Craessaerts, J.S. Mumm, E.H. Schroeter, V. Schrijvers, M.S. Wolfe, W.J. Ray, et al. 1999. A presenilin-1-dependent gamma-secretase-like protease mediates release of Notch intracellular domain. *Nature*. 398:518–522. http://dx.doi.org/10.1038/19083

Eckert, M.A., T.M. Lwin, A.T. Chang, J. Kim, E. Danis, L. Ohno-Machado, and J. Yang. 2011. Twist1-induced invadopodia formation promotes tumor metastasis. *Cancer Cell*. 19:372–386. http://dx.doi.org/10.1016/j.ccr.2011.01.036

Ellisen, L.W., J. Bird, D.C. West, A.L. Soreng, T.C. Reynolds, S.D. Smith, and J. Sklar. 1991. TAN-1, the human homolog of the *Drosophila* notch gene, is broken by chromosomal translocations in T lymphoblastic neoplasms. *Cell*. 66:649–661. http://dx.doi.org/10.1016/0092-8674(91)90111-B

Friedl, P., J. Locker, E. Sahai, and J.E. Segall. 2012. Classifying collective cancer cell invasion. *Nat. Cell Biol.* 14:777–783. http://dx.doi.org/10.1038/ncb2548

Fröhlich, C., R. Albrechtsen, L. Dyrskjøt, L. Rudkjaer, T.F. Ørntoft, and U.M. Wewer. 2006. Molecular profiling of ADAM12 in human bladder cancer. *Clin. Cancer Res.* 12:7359–7368. http://dx.doi.org/10.1158/1078-0432.CCR-06-1066

Garber, M.E., O.G. Troyanskaya, K. Schluens, S. Petersen, Z. Thaesler, M. Pacyna-Gengelbach, M. van de Rijn, G.D. Rosen, C.M. Perou, R.I. Whyte, et al. 2001. Diversity of gene expression in adenocarcinoma of the lung. *Proc. Natl. Acad. Sci. USA*. 98:13784–13789. http://dx.doi.org/10.1073/pnas.241500798

Goishi, K., S. Higashiyama, M. Klagsbrun, N. Nakano, T. Umata, M. Ishikawa, E. Mekada, and N. Taniguchi. 1995. Phorbol ester induces the rapid

processing of cell surface heparin-binding EGF-like growth factor: conversion from juxtacrine to paracrine growth factor activity. *Mol. Biol. Cell*. 6:967–980.

Guruharsha, K.G., M.W. Kankel, and S. Artavanis-Tsakonas. 2012. The Notch signalling system: recent insights into the complexity of a conserved pathway. *Nat. Rev. Genet.* 13:654–666. http://dx.doi.org/10.1038/nrg3272

Gustafsson, M.V., X. Zheng, T. Pereira, K. Gradin, S. Jin, J. Lundkvist, J.L. Ruas, L. Poellinger, U. Lendahl, and M. Bondesson. 2005. Hypoxia requires notch signaling to maintain the undifferentiated cell state. *Dev. Cell*. 9:617–628. http://dx.doi.org/10.1016/j.devcel.2005.09.010

Hanahan, D., and R.A. Weinberg. 2011. Hallmarks of cancer: the next generation. *Cell*. 144:646–674. http://dx.doi.org/10.1016/j.cell.2011.02.013

Higashiyama, S., J.A. Abraham, J. Miller, J.C. Fiddes, and M. Klagsbrun. 1991. A heparin-binding growth factor secreted by macrophage-like cells that is related to EGF. *Science*. 251:936–939. http://dx.doi.org/10.1126/science.1840698

Higashiyama, S., R. Iwamoto, K. Goishi, G. Raab, N. Taniguchi, M. Klagsbrun, and E. Mekada. 1995. The membrane protein CD9/DRAP 27 potentiates the juxtacrine growth factor activity of the membrane-anchored heparin-binding EGF-like growth factor. *J. Cell Biol.* 128:929–938. http://dx.doi.org/10.1083/jcb.128.5.929

Hiraga, T., S. Kizaka-Kondoh, K. Hirota, M. Hiraoka, and T. Yoneda. 2007. Hypoxia and hypoxia-inducible factor-1 expression enhance osteolytic bone metastases of breast cancer. *Cancer Res.* 67:4157–4163. http://dx.doi.org/10.1158/0008-5472.CAN-06-2355

Höckel, M., K. Schlenger, C. Knoop, and P. Vaupel. 1991. Oxygenation of carcinomas of the uterine cervix: evaluation by computerized O2 tension measurements. *Cancer Res.* 51:6098–6102.

Höckel, M., K. Schlenger, B. Aral, M. Mitze, U. Schaffer, and P. Vaupel. 1996. Association between tumor hypoxia and malignant progression in advanced cancer of the uterine cervix. *Cancer Res.* 56:4509–4515.

Hou, J., J. Aerts, B. den Hamer, W. van Ijcken, M. den Bakker, P. Riegman, C. van der Leest, P. van der Spek, J.A. Foekens, H.C. Hoogsteden, et al. 2010. Gene expression-based classification of non-small cell lung carcinomas and survival prediction. *PLoS ONE*. 5:e10312. http://dx.doi.org/10.1371/journal.pone.0010312

Hu, B., E. Castillo, L. Harewood, P. Ostano, A. Reymond, R. Dummer, W. Raffoul, W. Hoetzenecker, G.F. Hofbauer, and G.P. Dotto. 2012. Multifocal epithelial tumors and field cancerization from loss of mesenchymal CSL signaling. *Cell*. 149:1207–1220. http://dx.doi.org/10.1016/j.cell.2012.03.048

Keith, B., and M.C. Simon. 2007. Hypoxia-inducible factors, stem cells, and cancer. *Cell*. 129:465–472. http://dx.doi.org/10.1016/j.cell.2007.04.019

Kodama, T., E. Ikeda, A. Okada, T. Ohtsuka, M. Shimoda, T. Shiomi, K. Yoshida, M. Nakada, E. Ohuchi, and Y. Okada. 2004. ADAM12 is selectively overexpressed in human glioblastomas and is associated with glioblastoma cell proliferation and shedding of heparin-binding epidermal growth factor. *Am. J. Pathol.* 165:1743–1753. http://dx.doi.org/10.1016/S0002-9440(10)63429-3

Krishnan, J., P. Ahuja, S. Bodenmann, D. Knapik, E. Perriard, W. Krek, and J.C. Perriard. 2008. Essential role of developmentally activated hypoxia-inducible factor 1alpha for cardiac morphogenesis and function. *Circ. Res.* 103:1139–1146. http://dx.doi.org/10.1161/01.RES.0000338613.89841.c1

Kung, A.L., S. Wang, J.M. Klco, W.G. Kaelin, and D.M. Livingston. 2000. Suppression of tumor growth through disruption of hypoxia-inducible transcription. *Nat. Med.* 6:1335–1340. http://dx.doi.org/10.1038/82146

Kurisaki, T., A. Masuda, K. Sudo, J. Sakagami, S. Higashiyama, Y. Matsuda, A. Nagabukuro, A. Tsuji, Y. Nabeshima, M. Asano, et al. 2003. Phenotypic analysis of Meltrin alpha (ADAM12)-deficient mice: involvement of Meltrin alpha in adipogenesis and myogenesis. *Mol. Cell. Biol.* 23:55–61. http://dx.doi.org/10.1128/MCB.23.1.55-61.2003

Kveiborg, M., C. Fröhlich, R. Albrechtsen, V. Tischler, N. Dietrich, P. Holck, P. Kronqvist, F. Rank, A.M. Mercurio, and U.M. Wewer. 2005. A role for ADAM12 in breast tumor progression and stromal cell apoptosis. *Cancer Res.* 65:4754–4761. http://dx.doi.org/10.1158/0008-5472.CAN-05-0262

Landi, M.T., T. Dracheva, M. Rotunno, J.D. Figueroa, H. Liu, A. Dasgupta, F.E. Mann, J. Fukuoka, M. Hames, A.W. Bergen, et al. 2008. Gene expression signature of cigarette smoking and its role in lung adenocarcinoma development and survival. *PLoS ONE*. 3:e1651. http://dx.doi.org/10.1371/journal.pone.0001651

Lendeckel, U., J. Kohl, M. Arndt, S. Carl-McGrath, H. Donat, and C. Röcken. 2005. Increased expression of ADAM family members in human breast cancer and breast cancer cell lines. *J. Cancer Res. Clin. Oncol.* 131:41–48. http://dx.doi.org/10.1007/s00432-004-0619-y

Le Pabic, H., D. Bonnier, U.M. Wewer, A. Coutand, O. Musso, G. Baffet, B. Clément, and N. Théret. 2003. ADAM12 in human liver cancers: TGF-beta-regulated expression in stellate cells is associated with matrix remodeling. *Hepatology*. 37:1056–1066. http://dx.doi.org/10.1053/jhep.2003.50205

Lester, R.D., M. Jo, V. Montel, S. Takimoto, and S.L. Gonias. 2007. uPAR induces epithelial–mesenchymal transition in hypoxic breast cancer cells. *J. Cell Biol.* 178:425–436. http://dx.doi.org/10.1083/jcb.200701092

Li, H., E. Solomon, S. Duhachek Muggy, D. Sun, and A. Zolkiewska. 2011. Metalloprotease-disintegrin ADAM12 expression is regulated by Notch signaling via microRNA-29. *J. Biol. Chem.* 286:21500–21510. http://dx.doi.org/10.1074/jbc.M110.207951

Liao, D., C. Corle, T.N. Seagroves, and R.S. Johnson. 2007. Hypoxia-inducible factor-1alpha is a key regulator of metastasis in a transgenic model of cancer initiation and progression. *Cancer Res.* 67:563–572. http://dx.doi.org/10.1158/0008-5472.CAN-06-2701

Linder, S. 2007. The matrix corroded: podosomes and invadopodia in extracellular matrix degradation. *Trends Cell Biol.* 17:107–117. http://dx.doi.org/10.1016/j.tcb.2007.01.002

Linder, S., D. Nelson, M. Weiss, and M. Aepfelbacher. 1999. Wiskott-Aldrich syndrome protein regulates podosomes in primary human macrophages. *Proc. Natl. Acad. Sci. USA*. 96:9648–9653. http://dx.doi.org/10.1073/pnas.96.17.9648

Lucien, F., K. Brochu-Gaudreau, D. Arsenault, K. Harper, and C.M. Dubois. 2011. Hypoxia-induced invadopodia formation involves activation of NHE-1 by the p90 ribosomal S6 kinase (p90RSK). *PLoS ONE*. 6:e28851. http://dx.doi.org/10.1371/journal.pone.0028851

Maraver, A., P.J. Fernandez-Marcos, D. Herranz, M. Cañamero, M. Muñoz-Martin, G. Gómez-López, F. Mulero, D. Megías, M. Sanchez-Carbayo, J. Shen, et al. 2012. Therapeutic effect of γ-secretase inhibition in KrasG12V-driven non-small cell lung carcinoma by derepression of DUSP1 and inhibition of ERK. *Cancer Cell*. 22:222–234. http://dx.doi.org/10.1016/j.ccr.2012.06.014

Marchisio, P.C., D. Cirillo, L. Naldini, M.V. Primavera, A. Teti, and A. Zambonin-Zallone. 1984. Cell-substratum interaction of cultured avian osteoclasts is mediated by specific adhesion structures. *J. Cell Biol.* 99:1696–1705. http://dx.doi.org/10.1083/jcb.99.5.1696

Markowski, J., M. Oczko-Wojciechowska, T. Gierek, M. Jarzab, J. Paluch, M. Kowalska, Z. Wygoda, A. Pfeifer, T. Tyszkiewicz, B. Jarzab, et al. 2009. Gene expression profile analysis in laryngeal cancer by high-density oligonucleotide microarrays. *J. Physiol. Pharmacol.* 60(Suppl. 1):57–63.

Maxwell, P.H., G.U. Dachs, J.M. Gleadle, L.G. Nicholls, A.L. Harris, I.J. Stratford, O. Hankinson, C.W. Pugh, and P.J. Ratcliffe. 1997. Hypoxia-inducible factor-1 modulates gene expression in solid tumors and influences both angiogenesis and tumor growth. *Proc. Natl. Acad. Sci. USA*. 94:8104–8109. http://dx.doi.org/10.1073/pnas.94.15.8104

Mazure, N.M., E.Y. Chen, P. Yeh, K.R. Laderoute, and A.J. Giaccia. 1996. Oncogenic transformation and hypoxia synergistically act to modulate vascular endothelial growth factor expression. *Cancer Res.* 56:3436–3440.

Mino, N., R. Miyahara, E. Nakayama, T. Takahashi, A. Takahashi, S. Iwakiri, M. Sonobe, K. Okubo, T. Hirata, A. Sehara, and H. Date. 2009. A disintegrin and metalloprotease 12 (ADAM12) is a prognostic factor in resected pathological stage I lung adenocarcinoma. *J. Surg. Oncol.* 100:267–272. http://dx.doi.org/10.1002/jso.21313

Mitamura, T., S. Higashiyama, N. Taniguchi, M. Klagsbrun, and E. Mekada. 1995. Diphtheria toxin binds to the epidermal growth factor (EGF)-like domain of human heparin-binding EGF-like growth factor/diphtheria toxin receptor and inhibits specifically its mitogenic activity. *J. Biol. Chem.* 270:1015–1019. http://dx.doi.org/10.1074/jbc.270.3.1015

Miyamoto, S., M. Hirata, A. Yamazaki, T. Kageyama, H. Hasuwa, H. Mizushima, Y. Tanaka, H. Yagi, K. Sonoda, M. Kai, et al. 2004. Heparin-binding EGF-like growth factor is a promising target for ovarian cancer therapy. *Cancer Res.* 64:5720–5727. http://dx.doi.org/10.1158/0008-5472.CAN-04-0811

Mumm, J.S., E.H. Schroeter, M.T. Saxena, A. Griesemer, X. Tian, D.J. Pan, W.J. Ray, and R. Kopan. 2000. A ligand-induced extracellular cleavage regulates gamma-secretase-like proteolytic activation of Notch1. *Mol. Cell*. 5:197–206. http://dx.doi.org/10.1016/S1097-2765(00)80416-5

Murphy, D.A., and S.A. Courtneidge. 2011. The 'ins' and 'outs' of podosomes and invadopodia: characteristics, formation and function. *Nat. Rev. Mol. Cell Biol.* 12:413–426. http://dx.doi.org/10.1038/nrm3141

Murphy, D.A., B. Diaz, P.A. Bromann, J.H. Tsai, Y. Kawakami, J. Maurer, R.A. Stewart, J.C. Izpisúa-Belmonte, and S.A. Courtneidge. 2011. A Src-Tks5 pathway is required for neural crest cell migration during embryonic development. *PLoS ONE*. 6:e22499. http://dx.doi.org/10.1371/journal.pone.0022499

Ohh, M., C.W. Park, M. Ivan, M.A. Hoffman, T.Y. Kim, L.E. Huang, N. Pavletich, V. Chau, and W.G. Kaelin. 2000. Ubiquitination of hypoxia-inducible factor requires direct binding to the beta-domain of the von Hippel-Lindau protein. *Nat. Cell Biol.* 2:423–427. http://dx.doi.org/10.1038/35017054

Ongusaha, P.P., J.C. Kwak, A.J. Zwible, S. Macip, S. Higashiyama, N. Taniguchi, L. Fang, and S.W. Lee. 2004. HB-EGF is a potent inducer

of tumor growth and angiogenesis. *Cancer Res.* 64:5283–5290. http://dx.doi.org/10.1158/0008-5472.CAN-04-0925

Peduto, L., V.E. Reuter, A. Sehara-Fujisawa, D.R. Shaffer, H.I. Scher, and C.P. Blobel. 2006. ADAM12 is highly expressed in carcinoma-associated stroma and is required for mouse prostate tumor progression. *Oncogene*. 25:5462–5466. http://dx.doi.org/10.1038/sj.onc.1209536

Petcherski, A.G., and J. Kimble. 2000. Mastermind is a putative activator for Notch. *Curr. Biol.* 10:R471–R473. http://dx.doi.org/10.1016/S0960-9822(00)00577-7

Provot, S., D. Zinyk, Y. Gunes, R. Kathri, Q. Le, H.M. Kronenberg, R.S. Johnson, M.T. Longaker, A.J. Giaccia, and E. Schipani. 2007. Hif-1α regulates differentiation of limb bud mesenchyme and joint development. *J. Cell Biol.* 177:451–464. http://dx.doi.org/10.1083/jcb.200612023

Rocks, N., G. Paulissen, F. Quesada Calvo, M. Polette, M. Gueders, C. Munaut, J.M. Foidart, A. Noel, P. Birembaut, and D. Cataldo. 2006. Expression of a disintegrin and metalloprotease (ADAM and ADAMTS) enzymes in human non-small-cell lung carcinomas (NSCLC). *Br. J. Cancer*. 94:724–730.

Roepman, P., L.F. Wessels, N. Kettelarij, P. Kemmeren, A.J. Miles, P. Lijnzaad, M.G. Tilanus, R. Koole, G.J. Hordijk, P.C. van der Vliet, et al. 2005. An expression profile for diagnosis of lymph node metastases from primary head and neck squamous cell carcinomas. *Nat. Genet.* 37:182–186. http://dx.doi.org/10.1038/ng1502

Roy, R., S. Rodig, D. Bielenberg, D. Zurakowski, and M.A. Moses. 2011. ADAM12 transmembrane and secreted isoforms promote breast tumor growth: a distinct role for ADAM12-S protein in tumor metastasis. *J. Biol. Chem.* 286:20758–20768. http://dx.doi.org/10.1074/jbc.M110.216036

Rubin, J.S., A.M. Chan, D.P. Bottaro, W.H. Burgess, W.G. Taylor, A.C. Cech, D.W. Hirschfield, J. Wong, T. Miki, P.W. Finch, et al. 1991. A broad-spectrum human lung fibroblast-derived mitogen is a variant of hepatocyte growth factor. *Proc. Natl. Acad. Sci. USA*. 88:415–419. http://dx.doi.org/10.1073/pnas.88.2.415

Sahin, U., G. Weskamp, K. Kelly, H.M. Zhou, S. Higashiyama, J. Peschon, D. Hartmann, P. Saftig, and C.P. Blobel. 2004. Distinct roles for ADAM10 and ADAM17 in ectodomain shedding of six EGFR ligands. *J. Cell Biol.* 164:769–779. http://dx.doi.org/10.1083/jcb.200307137

Sahlgren, C., M.V. Gustafsson, S. Jin, L. Poellinger, and U. Lendahl. 2008. Notch signaling mediates hypoxia-induced tumor cell migration and invasion. *Proc. Natl. Acad. Sci. USA*. 105:6392–6397. http://dx.doi.org/10.1073/pnas.0802047105

Santagata, S., F. Demichelis, A. Riva, S. Varambally, M.D. Hofer, J.L. Kutok, R. Kim, J. Tang, J.E. Montie, A.M. Chinnaiyan, et al. 2004. JAGGED1 expression is associated with prostate cancer metastasis and recurrence. *Cancer Res.* 64:6854–6857. http://dx.doi.org/10.1158/0008-5472.CAN-04-2500

Seals, D.F., and S.A. Courtneidge. 2003. The ADAMs family of metalloproteases: multidomain proteins with multiple functions. *Genes Dev.* 17:7–30. http://dx.doi.org/10.1101/gad.1039703

Seals, D.F., E.F. Azucena Jr., I. Pass, L. Tesfay, R. Gordon, M. Woodrow, J.H. Resau, and S.A. Courtneidge. 2005. The adaptor protein Tks5/Fish is required for podosome formation and function, and for the protease-driven invasion of cancer cells. *Cancer Cell*. 7:155–165. http://dx.doi.org/10.1016/j.ccr.2005.01.006

Sethi, N., X. Dai, C.G. Winter, and Y. Kang. 2011. Tumor-derived JAGGED1 promotes osteolytic bone metastasis of breast cancer by engaging notch signaling in bone cells. *Cancer Cell*. 19:192–205. http://dx.doi.org/10.1016/j.ccr.2010.12.022

Sjöblom, T., S. Jones, L.D. Wood, D.W. Parsons, J. Lin, T.D. Barber, D. Mandelker, R.J. Leary, J. Ptak, N. Silliman, et al. 2006. The consensus coding sequences of human breast and colorectal cancers. *Science*. 314:268–274. http://dx.doi.org/10.1126/science.1133427

Stautz, D., A. Sanjay, M.T. Hansen, R. Albrechtsen, U.M. Wewer, and M. Kveiborg. 2010. ADAM12 localizes with c-Src to actin-rich structures at the cell periphery and regulates Src kinase activity. *Exp. Cell Res.* 316:55–67. http://dx.doi.org/10.1016/j.yexcr.2009.09.017

Stearman, R.S., L. Dwyer-Nield, L. Zerbe, S.A. Blaine, Z. Chan, P.A. Bunn Jr., G.L. Johnson, F.R. Hirsch, D.T. Merrick, W.A. Franklin, et al. 2005. Analysis of orthologous gene expression between human pulmonary adenocarcinoma and a carcinogen-induced murine model. *Am. J. Pathol.* 167:1763–1775. http://dx.doi.org/10.1016/S0002-9440(10)61257-6

Stransky, N., A.M. Egloff, A.D. Tward, A.D. Kostic, K. Cibulskis, A. Sivachenko, G.V. Kryukov, M.S. Lawrence, C. Sougnez, A. McKenna, et al. 2011. The mutational landscape of head and neck squamous cell carcinoma. *Science*. 333:1157–1160. http://dx.doi.org/10.1126/science.1208130

Su, L.J., C.W. Chang, Y.C. Wu, K.C. Chen, C.J. Lin, S.C. Liang, C.H. Lin, J. Whang-Peng, S.L. Hsu, C.H. Chen, and C.Y. Huang. 2007. Selection of DDX5 as a novel internal control for Q-RT-PCR from microarray data using a block bootstrap re-sampling scheme. *BMC Genomics*. 8:140. http://dx.doi.org/10.1186/1471-2164-8-140

Talbot, S.G., C. Estilo, E. Maghami, I.S. Sarkaria, D.K. Pham, P. O-charoenrat, N.D. Socci, I. Ngai, D. Carlson, R. Ghossein, et al. 2005. Gene expression profiling allows distinction between primary and metastatic squamous cell carcinomas in the lung. *Cancer Res.* 65:3063–3071.

Tang, X.H., S. Deng, M. Li, and M.S. Lu. 2012. The anti-tumor effect of cross-reacting material 197, an inhibitor of heparin-binding EGF-like growth factor, in human resistant ovarian cancer. *Biochem. Biophys. Res. Commun.* 422:676–680. http://dx.doi.org/10.1016/j.bbrc.2012.05.052

Tokumaru, S., S. Higashiyama, T. Endo, T. Nakagawa, J.I. Miyagawa, K. Yamamori, Y. Hanakawa, H. Ohmoto, K. Yoshino, Y. Shirakata, et al. 2000. Ectodomain shedding of epidermal growth factor receptor ligands is required for keratinocyte migration in cutaneous wound healing. *J. Cell Biol.* 151:209–220. http://dx.doi.org/10.1083/jcb.151.2.209

Vaupel, P., K. Schlenger, C. Knoop, and M. Höckel. 1991. Oxygenation of human tumors: evaluation of tissue oxygen distribution in breast cancers by computerized O2 tension measurements. *Cancer Res.* 51:3316–3322.

Wachi, S., K. Yoneda, and R. Wu. 2005. Interactome-transcriptome analysis reveals the high centrality of genes differentially expressed in lung cancer tissues. *Bioinformatics*. 21:4205–4208. http://dx.doi.org/10.1093/bioinformatics/bti688

Wang, F., C. Sloss, X. Zhang, S.W. Lee, and J.C. Cusack. 2007. Membrane-bound heparin-binding epidermal growth factor like growth factor regulates E-cadherin expression in pancreatic carcinoma cells. *Cancer Res.* 67:8486–8493. http://dx.doi.org/10.1158/0008-5472.CAN-07-0498

Wang, G.L., B.H. Jiang, E.A. Rue, and G.L. Semenza. 1995. Hypoxia-inducible factor 1 is a basic-helix-loop-helix-PAS heterodimer regulated by cellular O2 tension. *Proc. Natl. Acad. Sci. USA*. 92:5510–5514. http://dx.doi.org/10.1073/pnas.92.12.5510

Wang, N.J., Z. Sanborn, K.L. Arnett, L.J. Bayston, W. Liao, C.M. Proby, I.M. Leigh, E.A. Collisson, P.B. Gordon, L. Jakkula, et al. 2011. Loss-of-function mutations in Notch receptors in cutaneous and lung squamous cell carcinoma. *Proc. Natl. Acad. Sci. USA*. 108:17761–17766. http://dx.doi.org/10.1073/pnas.1114669108

Weaver, A.M. 2006. Invadopodia: specialized cell structures for cancer invasion. *Clin. Exp. Metastasis*. 23:97–105. http://dx.doi.org/10.1007/s10585-006-9014-1

Weng, A.P., A.A. Ferrando, W. Lee, J.P. Morris IV, L.B. Silverman, C. Sanchez-Irizarry, S.C. Blacklow, A.T. Look, and J.C. Aster. 2004. Activating mutations of NOTCH1 in human T cell acute lymphoblastic leukemia. *Science*. 306:269–271. http://dx.doi.org/10.1126/science.1102160

Wharton, K.A., K.M. Johansen, T. Xu, and S. Artavanis-Tsakonas. 1985. Nucleotide sequence from the neurogenic locus notch implies a gene product that shares homology with proteins containing EGF-like repeats. *Cell*. 43:567–581. http://dx.doi.org/10.1016/0092-8674(85)90229-6

Xing, F., H. Okuda, M. Watabe, A. Kobayashi, S.K. Pai, W. Liu, P.R. Pandey, K. Fukuda, S. Hirota, T. Sugai, et al. 2011. Hypoxia-induced Jagged2 promotes breast cancer metastasis and self-renewal of cancer stem-like cells. *Oncogene*. 30:4075–4086. http://dx.doi.org/10.1038/onc.2011.122

Xu, K.P., Y. Ding, J. Ling, Z. Dong, and F.S. Yu. 2004. Wound-induced HB-EGF ectodomain shedding and EGFR activation in corneal epithelial cells. *Invest. Ophthalmol. Vis. Sci.* 45:813–820. http://dx.doi.org/10.1167/iovs.03-0851

Yamada, D., K. Ohuchida, K. Mizumoto, S. Ohhashi, J. Yu, T. Egami, H. Fujita, E. Nagai, and M. Tanaka. 2007. Increased expression of ADAM 9 and ADAM 15 mRNA in pancreatic cancer. *Anticancer Res.* 27:793–799.

Yamaguchi, H., M. Lorenz, S. Kempiak, C. Sarmiento, S. Coniglio, M. Symons, J. Segall, R. Eddy, H. Miki, T. Takenawa, and J. Condeelis. 2005. Molecular mechanisms of invadopodium formation: the role of the N-WASP–Arp2/3 complex pathway and cofilin. *J. Cell Biol.* 168:441–452. http://dx.doi.org/10.1083/jcb.200407076

Yang, Y., Y.H. Ahn, D.L. Gibbons, Y. Zang, W. Lin, N. Thilaganathan, C.A. Alvarez, D.C. Moreira, C.J. Creighton, P.A. Gregory, et al. 2011. The Notch ligand Jagged2 promotes lung adenocarcinoma metastasis through a miR-200-dependent pathway in mice. *J. Clin. Invest.* 121:1373–1385. http://dx.doi.org/10.1172/JCI42579

Young, S.D., R.S. Marshall, and R.P. Hill. 1988. Hypoxia induces DNA overreplication and enhances metastatic potential of murine tumor cells. *Proc. Natl. Acad. Sci. USA*. 85:9533–9537. http://dx.doi.org/10.1073/pnas.85.24.9533

Zavadil, J., L. Cermak, N. Soto-Nieves, and E.P. Böttinger. 2004. Integration of TGF-beta/Smad and Jagged1/Notch signalling in epithelial-to-mesenchymal transition. *EMBO J.* 23:1155–1165. http://dx.doi.org/10.1038/sj.emboj.7600069

Zeng, Q., S. Li, D.B. Chepeha, T.J. Giordano, J. Li, H. Zhang, P.J. Polverini, J. Nor, J. Kitajewski, and C.Y. Wang. 2005. Crosstalk between tumor and endothelial cells promotes tumor angiogenesis by MAPK activation of Notch signaling. *Cancer Cell*. 8:13–23. http://dx.doi.org/10.1016/j.ccr.2005.06.004